SUPPLEMENT No. 522

Huss Mikael:

Simulation of the capsize. MV ESTONIA Accident Investigation.

Internal report 1995 - 1997.

MV ESTONIA Accident Investigation
Internal Report
1995-1997

Simulation of the capsize

by
Mikael Huss

1 Summary

This report has been made in order to verify if the capsize scenario, as described by witnesses on board MV ESTONIA, can be reasonably explained by the loss of the bow visor, the opening of the forward ramp and the subsequent flooding of car deck.

The analysis concerns only the first phase of the capsize, before water started to enter the upper decks of the vessel. It is made in three different stages described in the separate sections of the report:

Floating condition and stability
The floating condition and quasi-static residual stability have been calculated for the first phase of the capsize when water was accumulating on the A-deck (car deck).
The calculations give input to the simulation of water inflow rate.

As is well known, a ship like the ESTONIA with a fully open vehicle deck is extremely sensitive to ingress of water. A relative small amount of water like 1000 ton (0.3 m water on the deck) will result in a heel angle of over 20°. Such a large heel will cause severe damage to the interior of the public areas, significant shift of vehicles and cargo, and presumably panic among the passengers. However, the water on the car deck is in itself not sufficient to make the ship capsize as long as the hull is intact below and above the open deck. The capsize is fulfilled only when water starts entering other areas of the ship. According to the hydrostatic calculations, this condition appears when 1500-2000 ton has entered the A-deck and the heel angle is in the range of 35°-40°. Apparently there have also been some water leaking down through the centre casing doors before the flooding of upper decks. However, this is believed to have had no significant effect on the stability or heeling of the vessel.

Relative motions at the bow
The vertical relative motions between the bow and the waves have been calculated with linear strip theory for the intact ship. Approximate calculations have also been made for two heeled conditions. The result show that the motions are very sensitive to the mean period of the wave spectrum and to the relative heading of the ship towards the waves. The influence of speed is less significant in the present condition. The relative motions for heeled conditions are generally smaller than for the intact ship in head and bow sea but similar or larger in beam sea.

Simulation of water inflow
The rate and time sequence of water inflow have been simulated from the frequency distribution of relative vertical motion amplitudes. The simulation takes into account the changed floating condition, heading and speed as estimated from manoeuvring simulations and witnesses statements. The results show that the assumed probable time sequence well can be verified by the simulations. However, the uncertainty in estimates is large and the time sequence is shown to be very sensitive to small changes in the condition.

2 Floating condition and stability

The hydrostatics characteristic of ESTONIA has been calculated with the program HYSS developed by the author. The calculation method has been verified in several independent comparisons with other well known commercial program systems. The ship geometry is modelled with a number of transverse sections, to which can be added or subtracted external or internal compartments.

Figure 2.1 shows the base model of the ESTONIA hull. A separate geometry model has been used for the car deck in the calculations of flooded conditions.

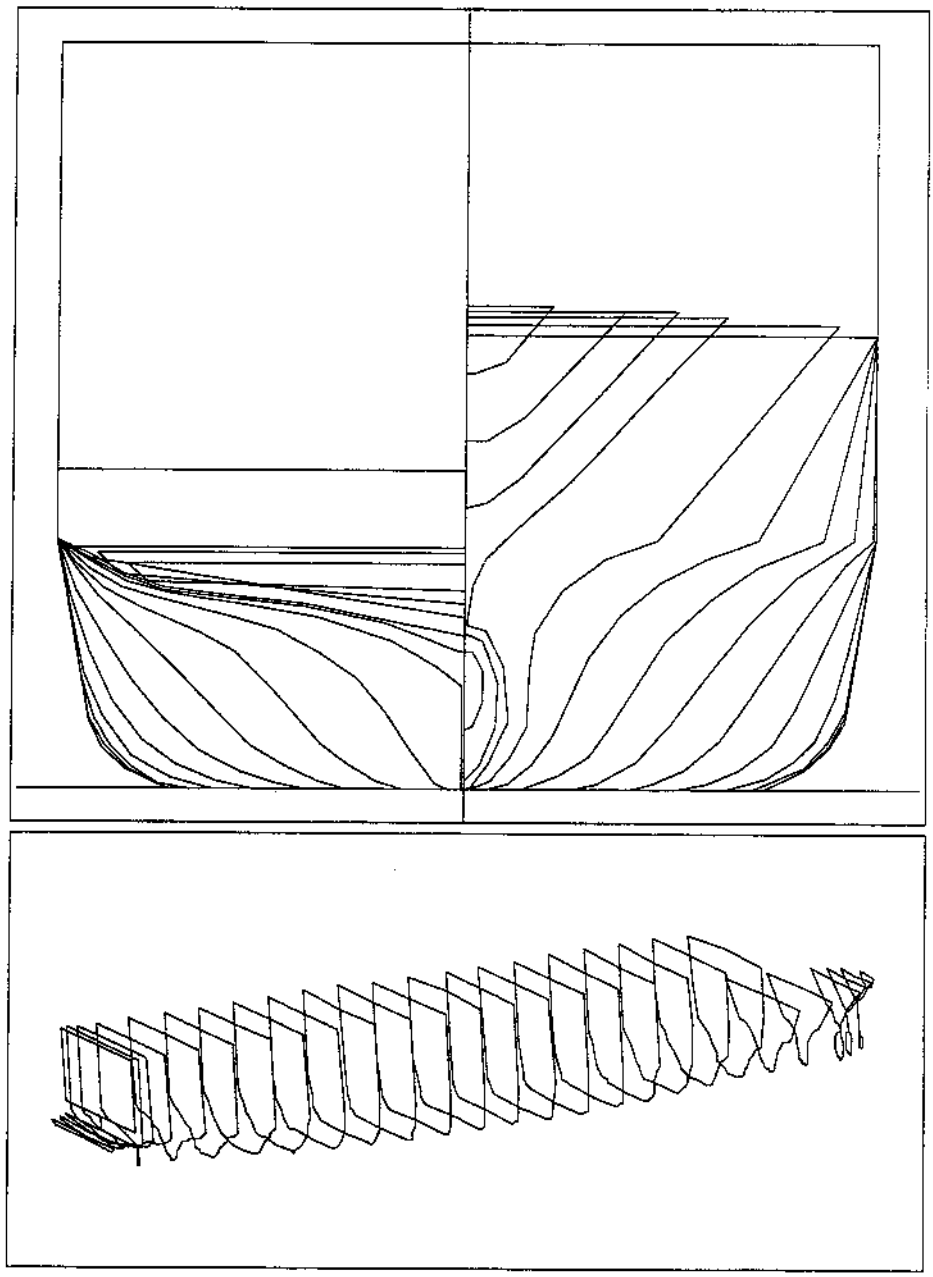

Figure 2.1 Hull geometry model of the ESTONIA used for hydrostatic calculations

2.1 Condition before flooding of car deck

The intact condition is taken from previous calculations with the NAPA program reported in [1].

Intact Condition

Displacement	12050 ton (11931 m^3 with an assumed density of 1.010 ton/m^3)
LCG	63.85 m fwd AP
KG	10.62 m

All calculations in this report refer to the conditions after the stem visor had left the ship. The weight of the visor is here assumed to be approximately 60 ton.

Damaged condition (before flooding)

Displacement	11990 ton
LCG	63.47 m fwd AP
KG	10.61 m

It is further assumed that no significant free surfaces were present except for the flooded car deck. This assumption gives a little over estimation of the initial stability (GM') but it is considered to be of no importance for the purpose of this study.

Main hydrostatic data for the intact and damaged condition is given in Table 2.1 below. A comparison with the intact floating condition calculated by HYSS and by NAPA [1], shows a difference of 0.020 m in draught and 0.013 m in trim. This difference is small and well within the uncertainty margin of the actual loading condition.

Dens SW = 1.010 ton/m^3		*Intact*	*Damaged*
Displacement SW	(ton):	12 050.00	11 990.00
LCG fw AP	(m):	63.850	63.470
TCG ps CL	(m):	0.000	0.000
KG	(m):	10.620	10.610
Equilibrium at:			
Draught mld at L/2	(m):	5.370	5.336
Trim (pos aft)	(m):	0.448	0.633
Heel a (pos ps)	(deg):	0.00	0.00
Displacement vol	(m^3):	11 930.66	11 871.30
LCB fw AP	(m):	63.828	63.434
TCB ps CL	(m):	0.000	0.000
KB	(m):	2.902	2.891
Waterplane Area	(m^2):	2 798.067	2 807.91
LCF fw AP	(m):	59.479	58.960
TCF ps CL	(m):	0.000	0.000
KF	(m):	5.400	5.380
BM - transv	(m):	8.958	9.047
KN - transv	(m):	0.000	0.000
BM - longit	(m):	306.988	311.77
Wetted Surface	(m^2):	3 687.457	3 691.06
GZ	(m):	0.000	0.000
dGZ/da	(m/rad):	1.240	1.328

Table 2.1 Main hydrostatic data before flooding for intact and damaged condition.

2.2 Effect of water inflow on A-deck

Floating conditions as function of the amount of water on A-deck have been calculated for the ship with C-deck intact and with C-deck and above open to flooding respectively. The later condition simulates the final part of the capsize when water has been reported entering accommodation decks by windows and aft doors.

In all calculations, the water on A-deck is allowed to flow freely to static equilibrium within the defined deck volume. The final equilibrium floating condition of the ship and the water distribution on A deck is solved by iteration. The A-deck has been modelled with the non-symmetric centre casing assumed to be intact. The permeability of car deck is assumed to be 90%. The influence from the permeability on the floating condition is however found to be rather small.

Figures 2.2-2.3 show examples of static stability curves (GZ) for different amount of water on A-deck. Figure 2.4 shows the stability curve for the condition of free flooding of all decks above A-deck. The results are close to the results presented in ref [1]. Floating equilibrium conditions in terms of heel, initial stability, draught and trim for different amount of water on A-deck is presented in Figures 2.5 - 2.8.

There has not been any attempt to model the flooded condition in the later stage of the capsize. When water starts entering the C-deck (i.e. the passenger deck above car decks), the ship is predestined to sink. The stability curves show that if the decks above car deck would have been water tight, the ship would probably have continued to float with a heel angle less then 50° at least for a significant period of time.

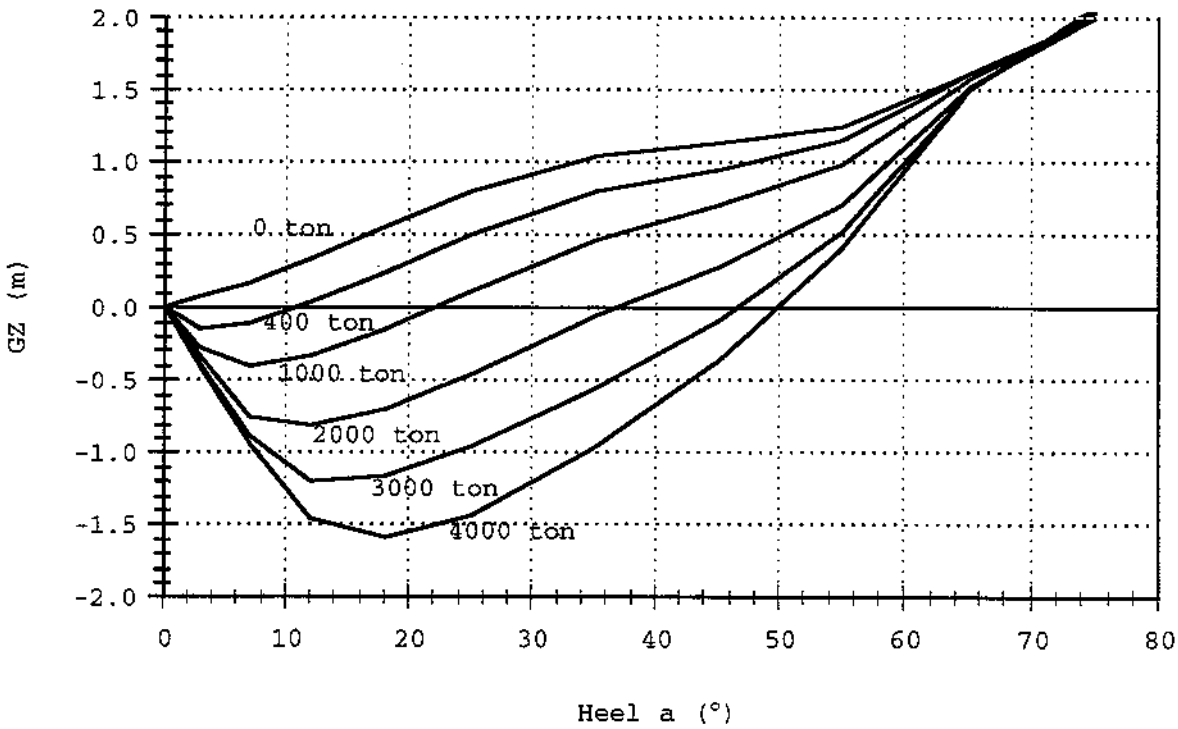

Figure 2.2 Static stability curves for different amount of water on A-deck. Volume permeability of A deck 0.90. C-deck and above intact.

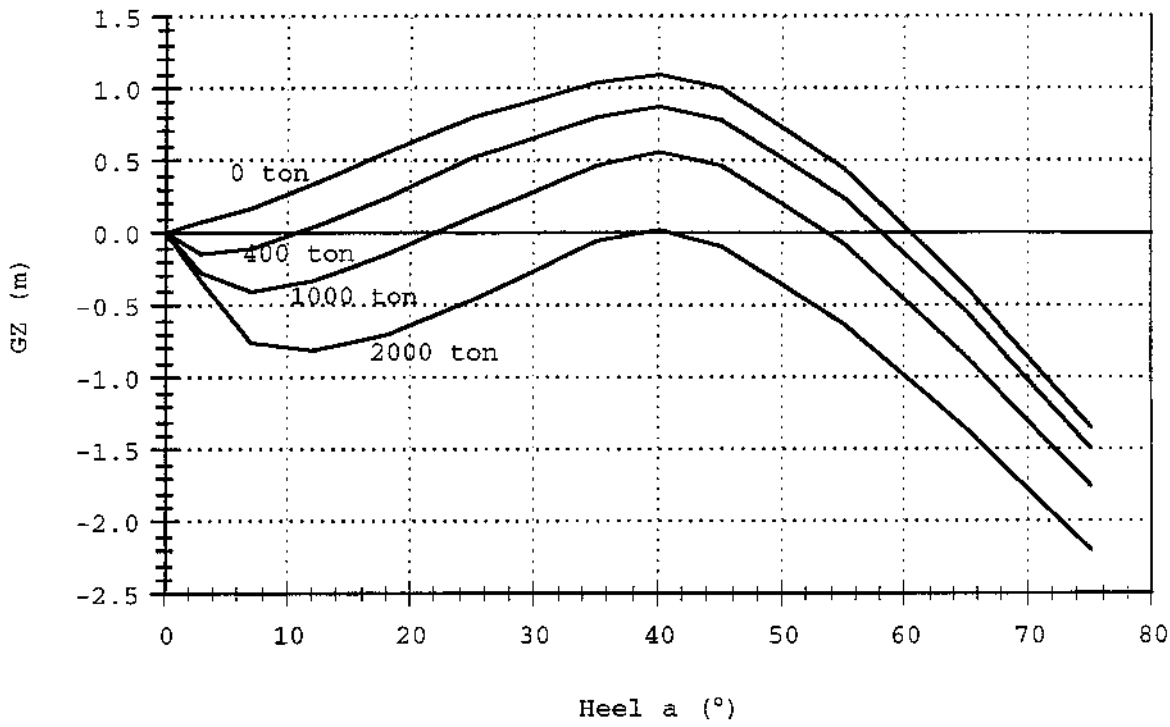

Figure 2.3 Static stability curves for different amount of water on A-deck.
Volume permeability of A deck 0.9.
C-deck and above open to free flooding (permeability 1.0).

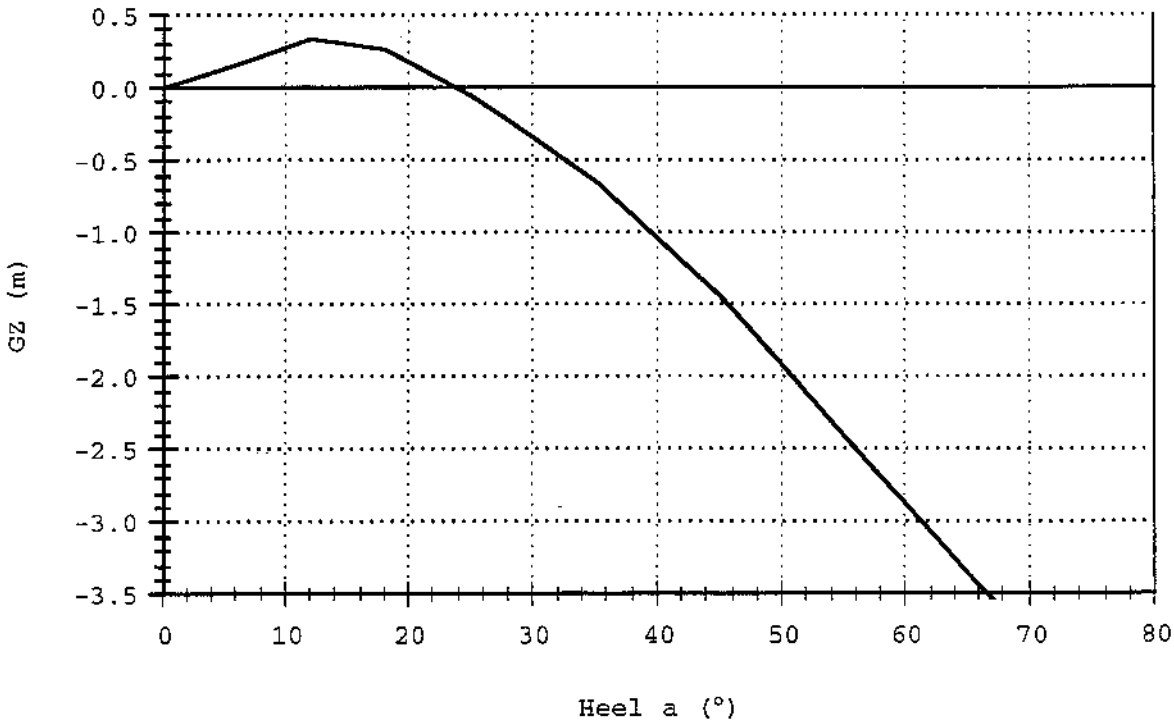

Figure 2.4 Static stability curves for A-deck and above open to free flooding.

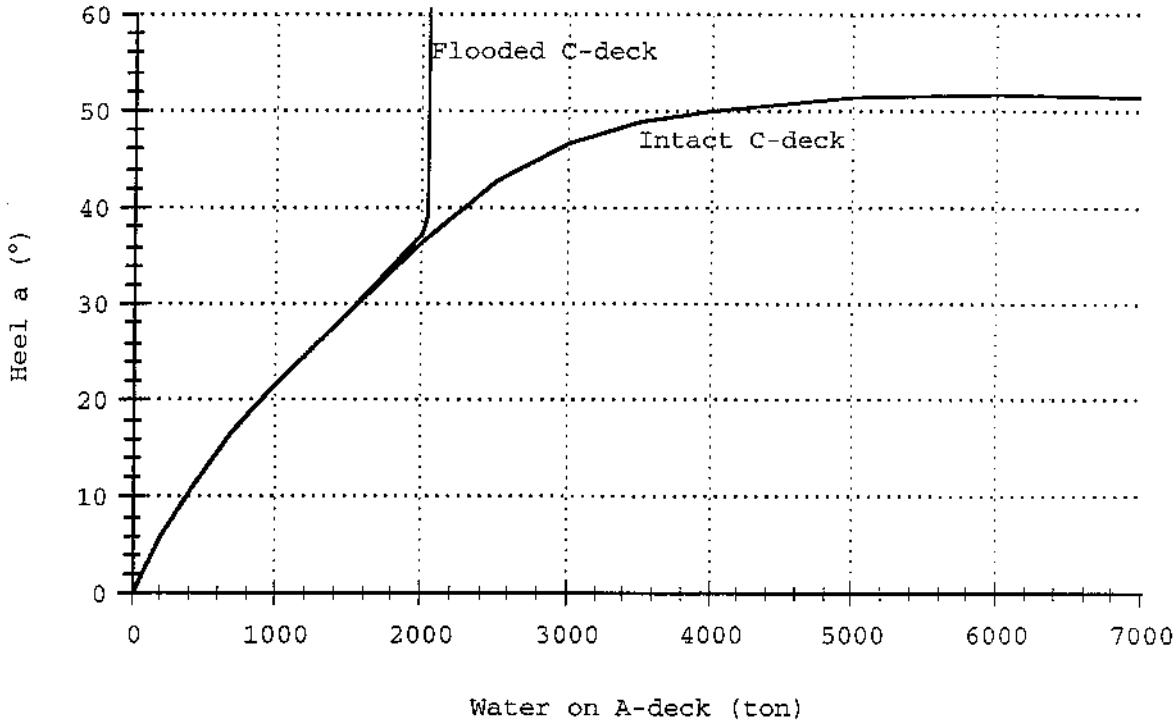

Figure 2.5 Heel angle at static equilibrium as function of water on A-deck

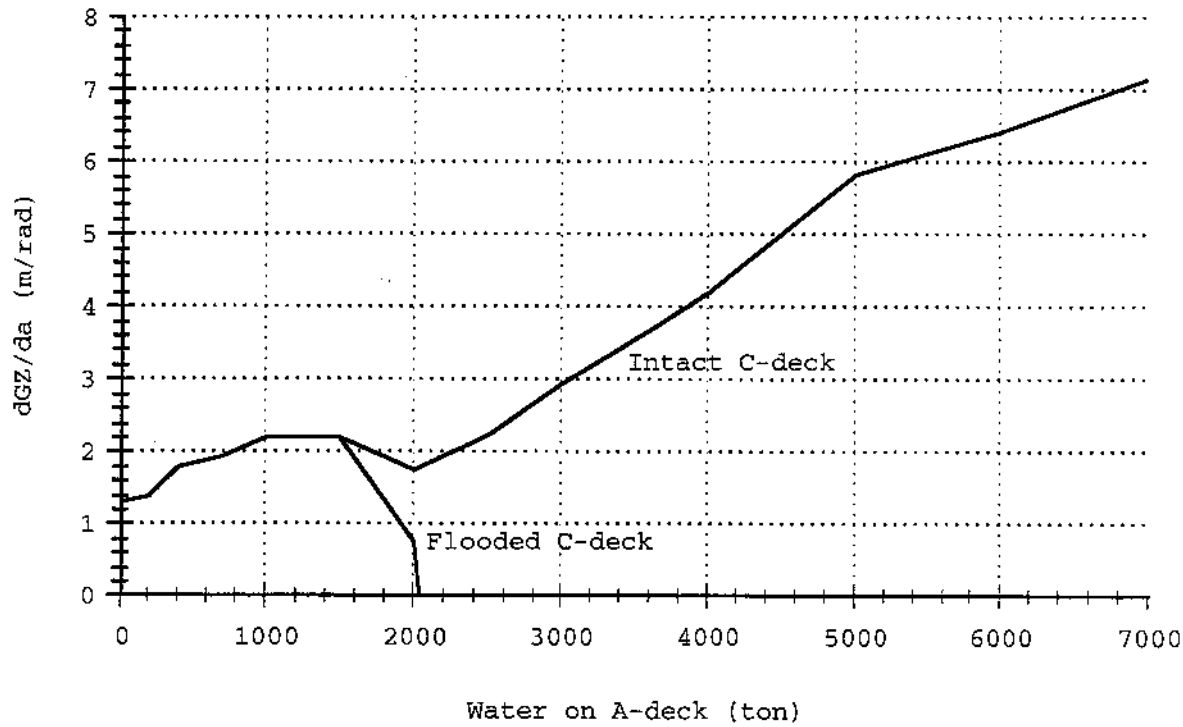

Figure 2.6 Stability derivate (initial stability) at heeled equilibrium condition as function of water on A-deck

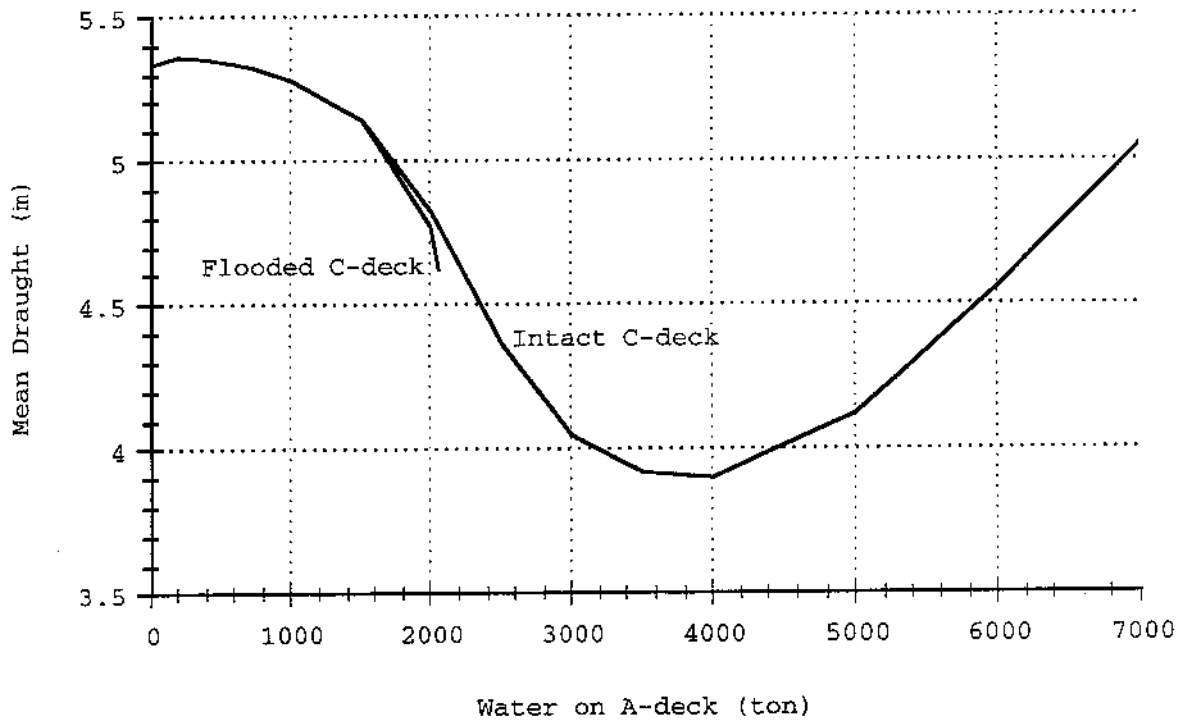

Figure 2.7 Mean draught (amidships at CL) at static equilibrium as function of water on A-deck

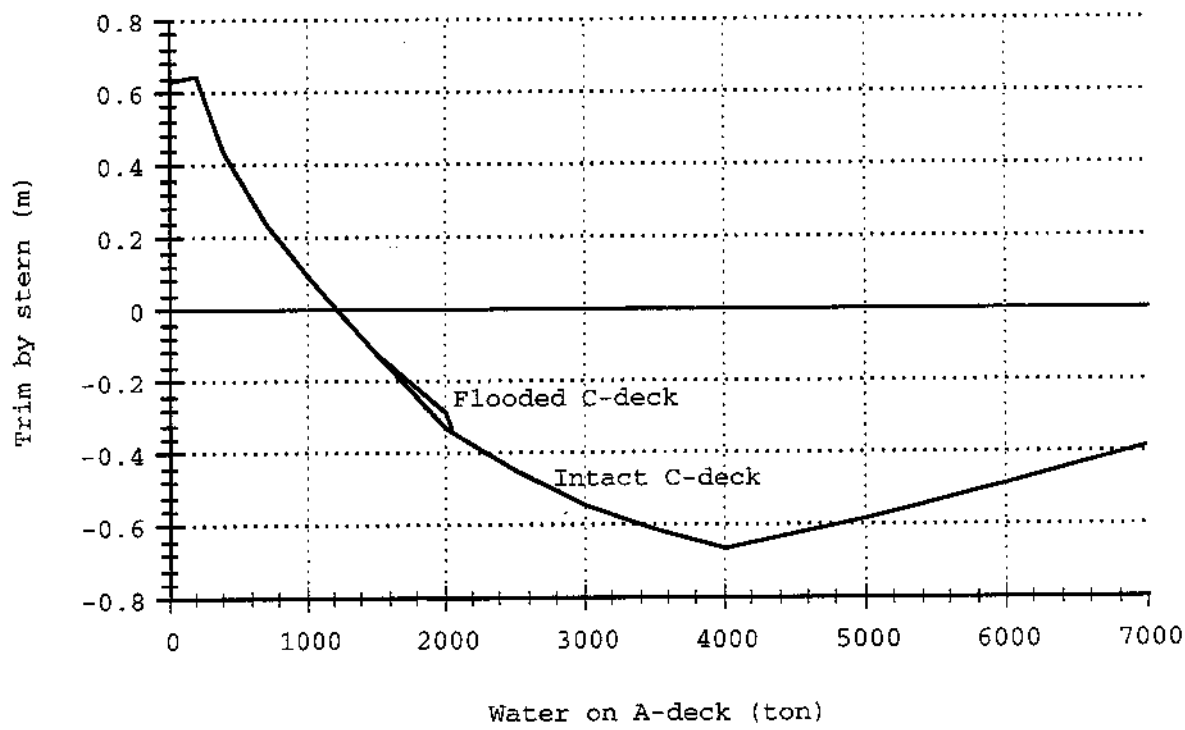

Figure 2.8 Trim by stern (at CL) at static equilibrium as function of water on A-deck

2.3 Influence of permeability and cargo shifting on A-deck

The filling rate or permeability of the cargo space will also have some effect on the stability characteristics during flooding. An assumed low permeability will result in lower heeling moments but at the same time in higher centre of gravity of the water. These two effects works contradictory, and the combined effect is very small. Figure 2.9 shows the effect of permeability on the static equilibrium heel angle. In all the previous figures, the permeability of car deck is assumed to be 0.9 and of the accommodation area 1.0.

It is very difficult to ascertain how shifting of vehicles and cargo on car deck developed during the water inflow. The weight of all vehicles have been estimated to about 1070 ton in total. The maximum transverse shift is of the order of one or a few meter. Every 1.1 m of cargo shift would have the effect of 0.1 m shift of the ships total centre of gravity. The resulting effect on the static stability curves is illustrated in Figures 2.10 and 2.11 for intact C-deck and open C-deck respectively.

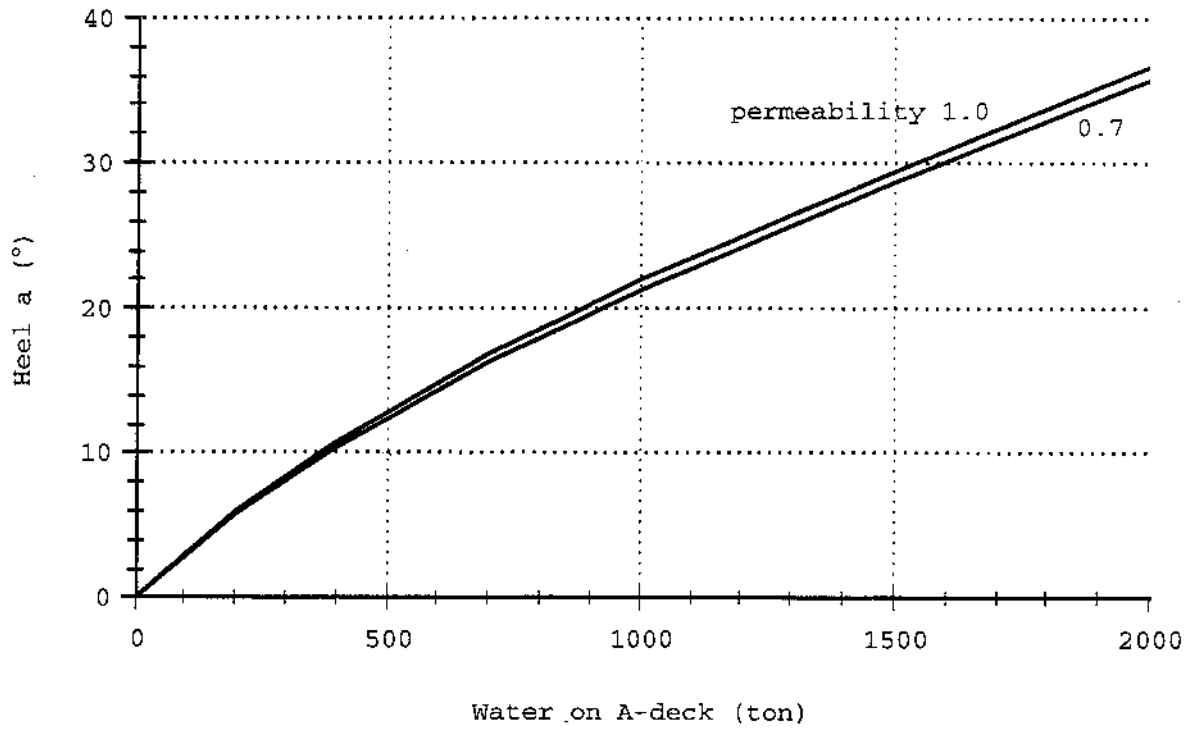

Figure 2.9 Heel angle at static equilibrium as function of water on A-deck. Effect of different assumptions of volume permeability

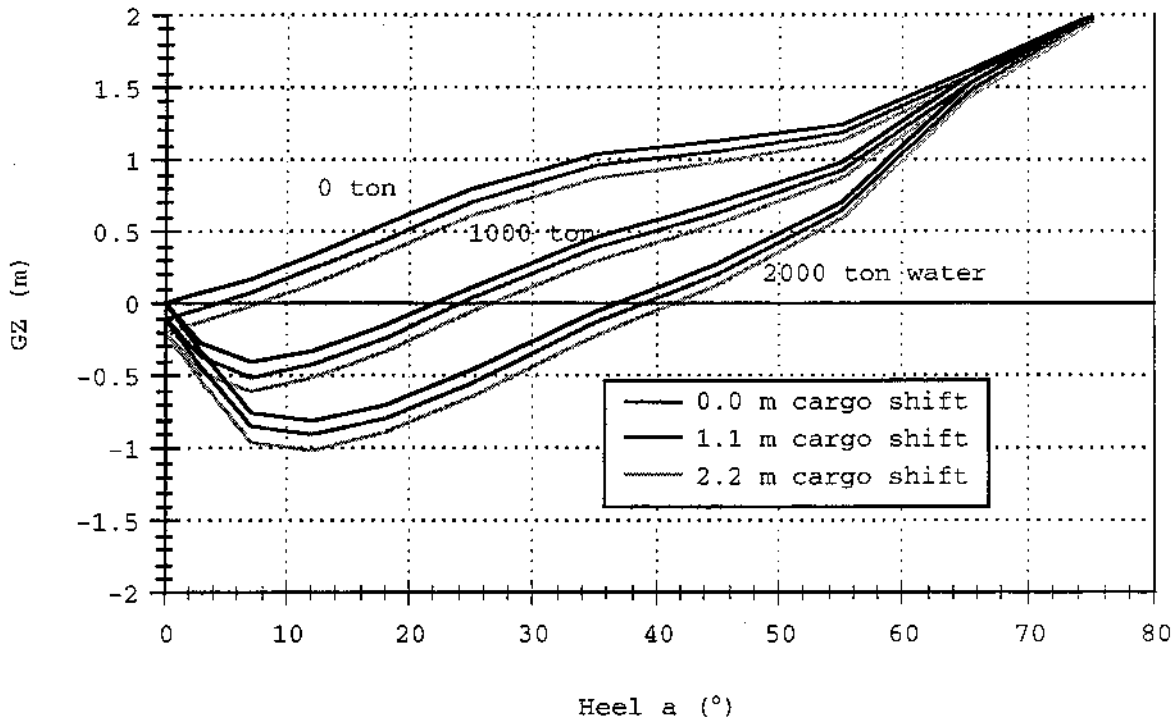

Figure 2.10 Effect of cargo shifting on static stability curves. C-deck and above intact.

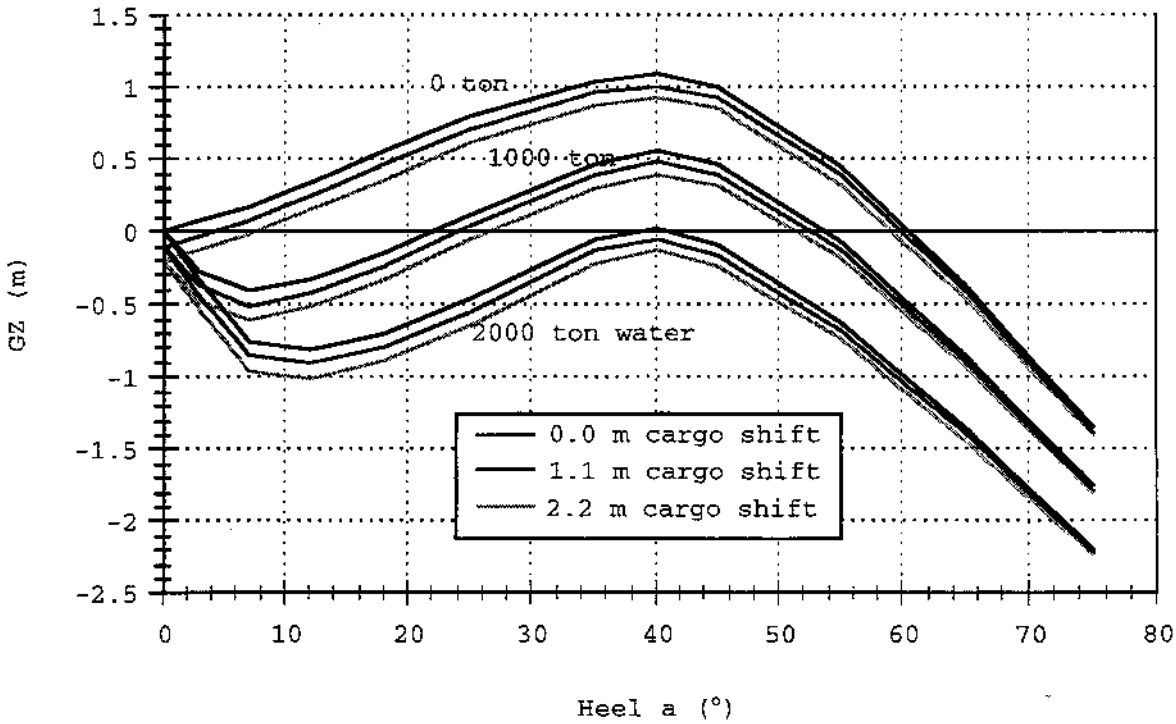

Figure 2.11 Effect of cargo shifting on static stability curves.
C-deck and above open to free flooding.

3 Relative motions at the bow

The statistical distribution of relative vertical motions between the ship bow and waves has been calculated with linear strip theory (Salvesen et al 1979). The sectional geometries were represented by 3-parameter Lewis transformations. For ordinary ship hull forms in upright/symmetric condition, this is a well established method that has been shown to give accurate results.

In an attempt to study the influence of water ingress on the relative motions, the same method has here also been used for heeled conditions. The transformation is in this case based on the heeled waterline breadth, the sectional area and the maximum draught measured perpendicular to the undisturbed waterline at each section. The non-symmetric geometry of the heeled sections is not taken into account, neither is the influence of the dynamics of the water entered into the ship. The results must therefore bee seen as rough estimates, but are believed to be reasonable accurate for the purpose of this study.

All calculations were performed with a general Naval Architecture program system 'MacSkepps' developed at KTH.

Figures 3.1-3.3 show the transformed geometry of the intact ship, and of the ship in equilibrium heeled condition with 1000 ton and 2000 ton water on A-deck respectively.

All calculations have been made for irregular seas using the JONSWAP wave spectrum with a peak magnifying factor of 3.3 to represent the frequency distribution.

Examples of calculated relative motion at the bow of the intact ship as function of speed and spectrum peak period, Tp, is shown in Figure 3.4. The results are very close to the results obtained from calculations with the linear strip theory according to Raff presented in reference [2], Fig. A.7, Fig. A.13.

A comparison of the response in long-crested and short-crested sea is shown in Figure 3.5. For the purpose of water inflow simulations as described in the next section, the motion response in short-crested waves have been used. The directional spreading is modelled with a $\cos^4$ -spreading function which is rather narrow and gives results in between the more broader $\cos^2$ - spreading function and long-crested waves.

Examples of calculated relative vertical motions at the bow for different speed, wave heading and amount of water on A-deck is given in Figures 3.6-3.9.

The influence of speed is not very significant. The flooded and heeled conditions in bow and head sea result in a reduction of the relative motions. The lowest relative motions appear in beam seas where the motion amplitudes approaches the wave amplitudes, i.e. the ratio rs/Hs is close to 0.5. Here rs is significant single amplitude relative vertical motion and Hs is significant wave height (double amplitude).

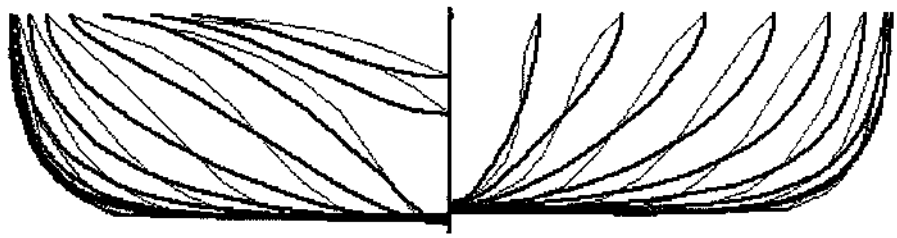

Figure 3.1 Comparison between transformed geometry and actual hull geometry, intact condition. (Bold lines show transformed geometry)

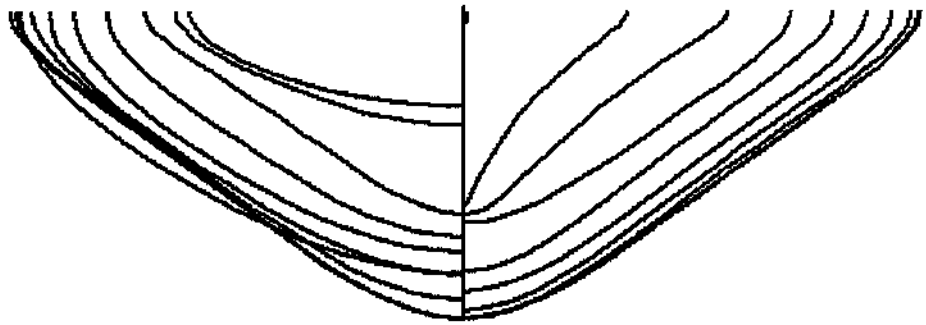

Figure 3.2 Transformed geometry for flooded condition
1000 ton water on A-deck, 22° heel

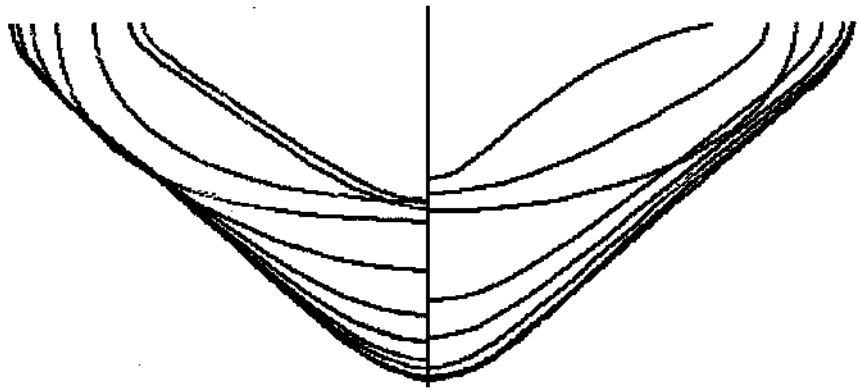

Figure 3.3 Transformed geometry for flooded condition
2000 ton water on A-deck, 37° heel

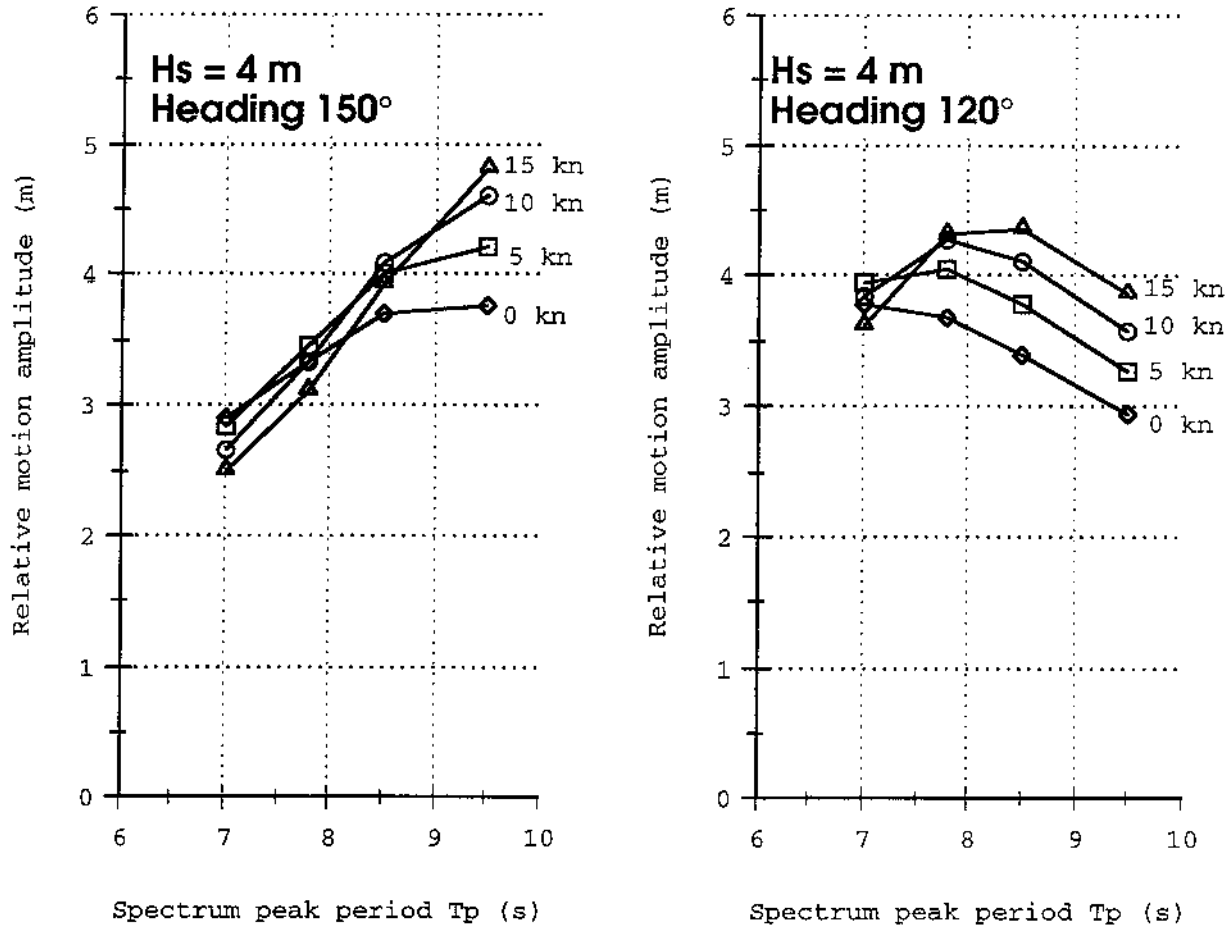

Figure 3.4 Relative vertical motion at bow in bow seas, long-crested waves

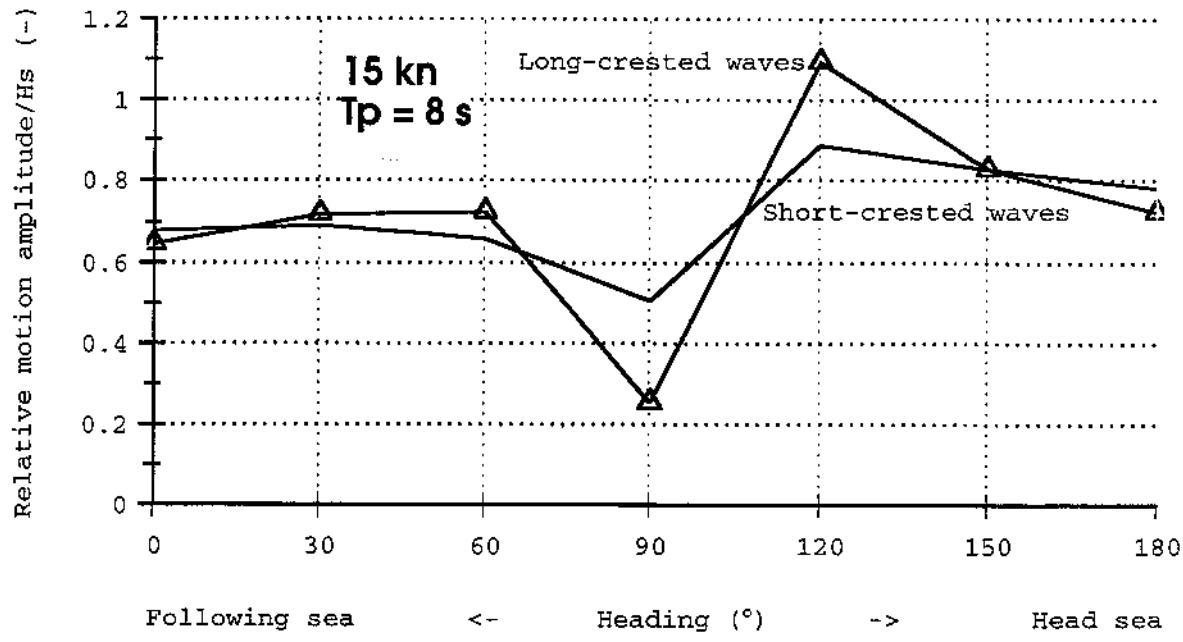

Figure 3.5 Comparison between long-crested and short-crested wave representation

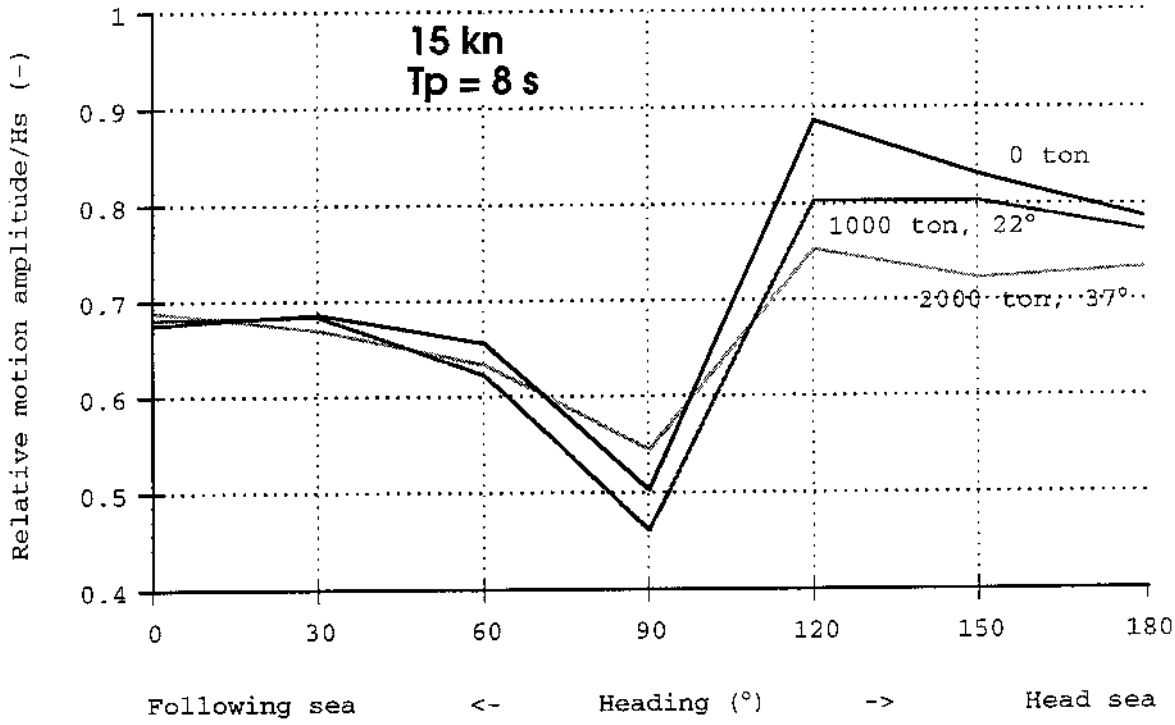

Figure 3.6 Non-dimensional relative vertical motion at bow as function of heading and amount of water on A-deck. 15 knots, Tp 8.0 s, short-crested waves.

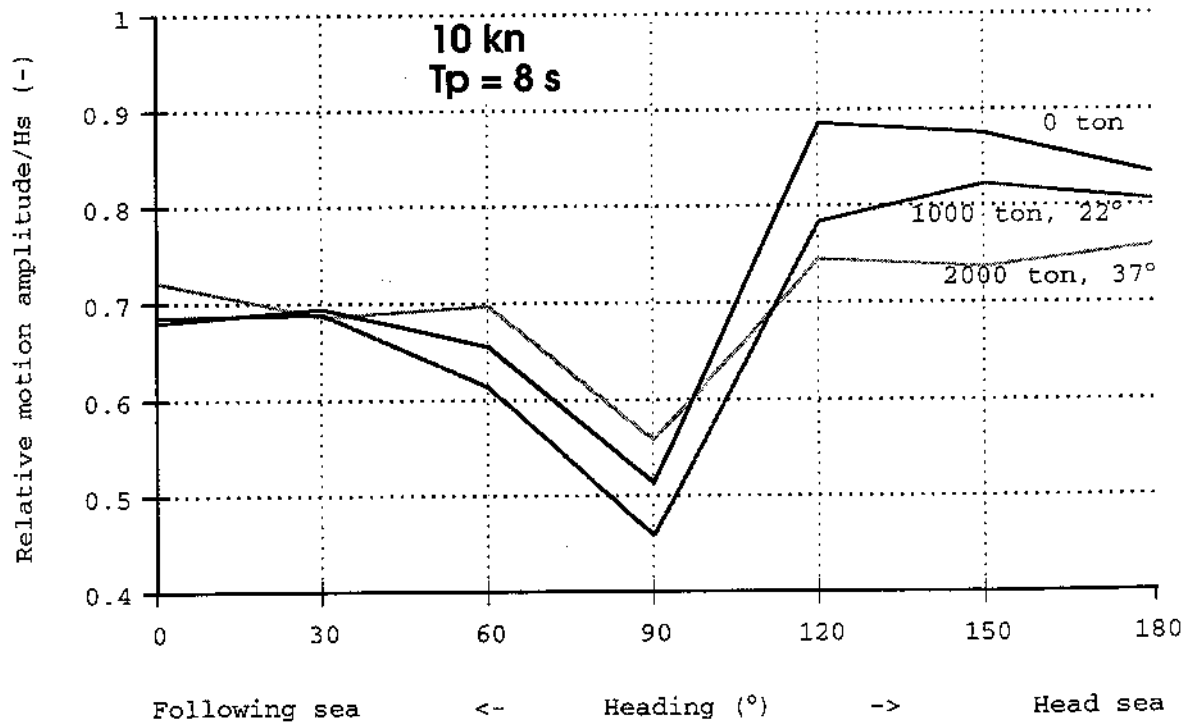

Figure 3.7 Non-dimensional relative vertical motion at bow as function of heading and amount of water on A-deck. 10 knots, Tp 8.0 s, short-crested waves.

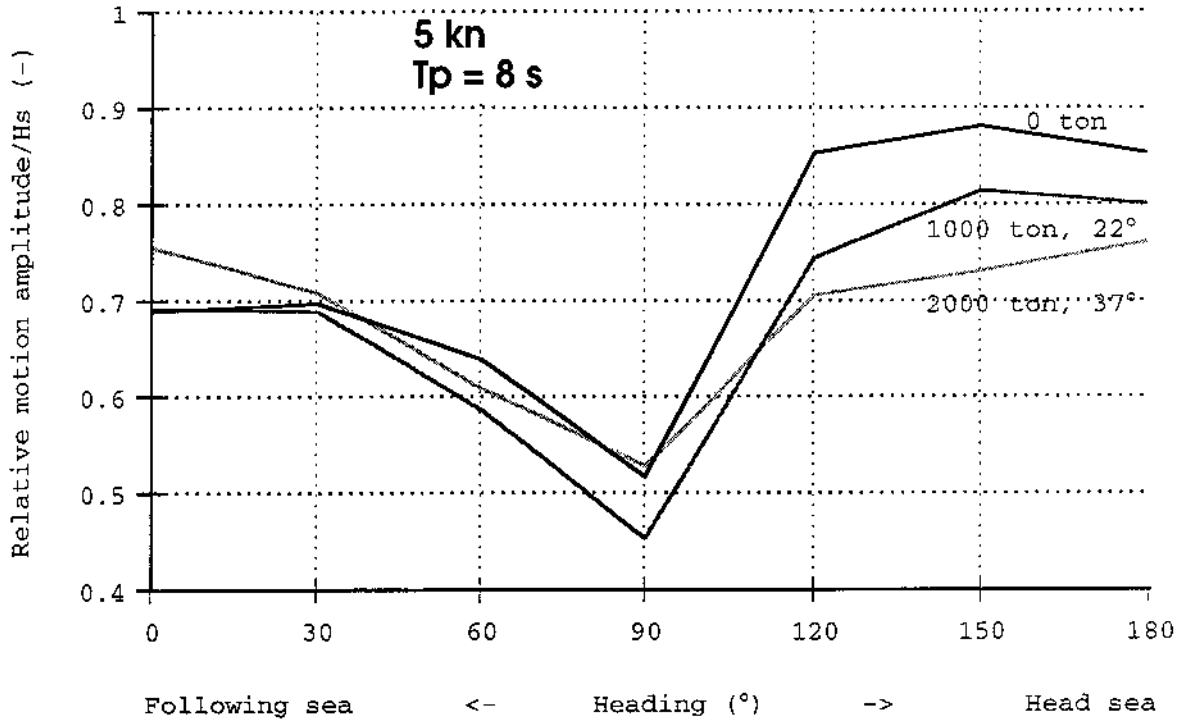

Figure 3.8 Non-dimensional relative vertical motion at bow as function of heading and amount of water on A-deck. 5 knots, Tp 8.0 s, short-crested waves.

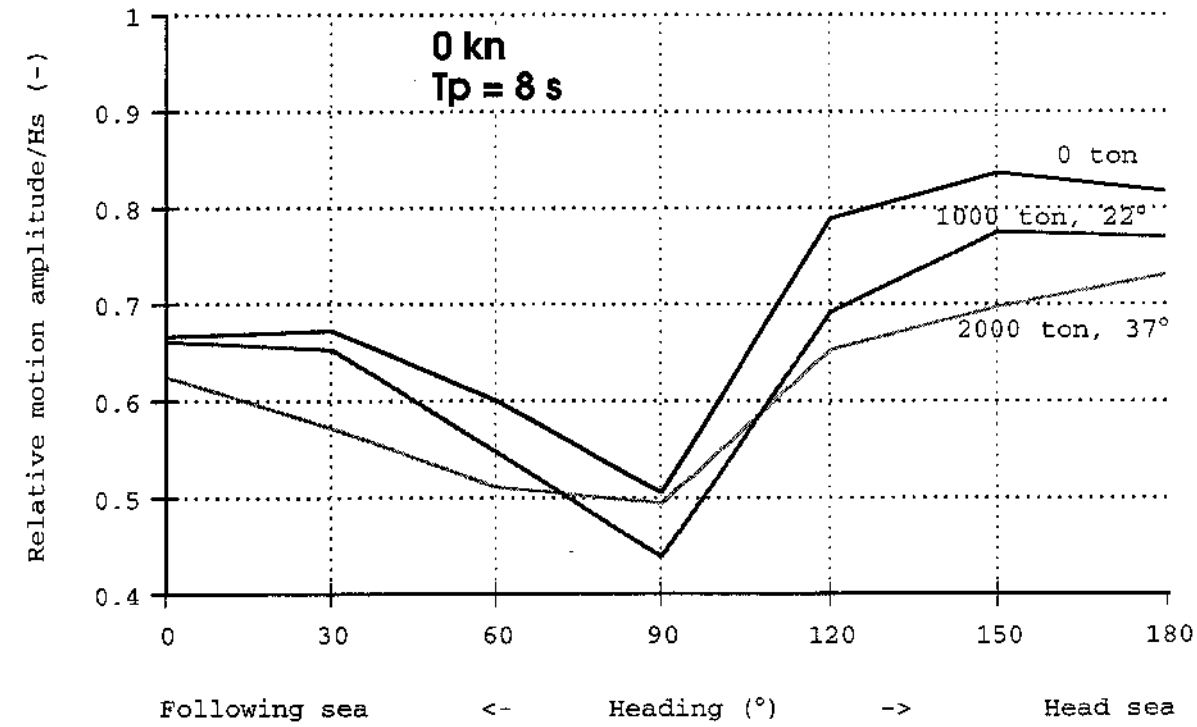

Figure 3.9 Non-dimensional relative vertical motion at bow as function of heading and amount of water on A-deck. 0 knots, Tp 8.0 s, short-crested waves.

4 Simulation of water inflow

The water inflow through the ramp opening when the visor was lost and the ramp torn open, has been estimated from the frequency distribution of the relative motion. The simulation was made on the basis of the previous described calculations of static equilibrium floating conditions and significant relative motions.

The results obtained from the simulations are very sensitive to small changes in the initial parameters and the inherent uncertainty in the random nature of waves and ship motions during short periods of time is very large. Therefore, this simulation (or any other) cannot be used to independently prove a certain time sequence. On the contrary, one important input to the simulation was actually a presumed time sequence. So the purpose of the simulation is mainly to verify whether an assumed capsizing scenario is likely to have happened or not.

4.1 Methods and assumptions

The general equation describing the water inflow in this simulation is formulated as:

$$Q_W(W,V_s,\beta,rs) = \int_{F(W)}^{\infty} \int_{F(W)}^{H(W)} V_W(z,r,W,V_s,\beta) \cdot b(z,W) \cdot f_r(r,rs)\, dzdr$$

with the following definitions:

$Q_W(W,V_s,\beta,rs)$	Mean volume of water inflow per second, (m^3/s)
W	Amount of accumulated water on A-deck, (ton) (Decisive for the heel and the draught at the bow)
V_S	Ship speed (m/s)
β	Ships heading relative to the waves, (°), (180° for head waves)
rs	Significant relative vertical motion at the bow opening, (m) (rs is a function of both the sea condition and the ship condition)
F(W)	Distance from the mean water level to the lowest corner of the ramp opening, (m)
H(W)	Height of the ramp opening measured perpendicular from the mean water surface, (m)
$V_W(z,r,W,V_s,\beta)$	Velocity of water inflow, (m/s)

z	Vertical ship coordinate defined from the still water line, (m)
r	Relative motion between wave surface and ship bow, (m) defined from the still water line
b(z,W)	Breadth of ramp opening at position z, (m)
$f_r(r,rs)$	Frequency distribution of relative motion, (1/m)

Definitions of z, F(W), H(W) and b(z,W) is shown in Figure 4.1.

The inflow velocity at a certain position z is approximated with the following expression:

when $r \geq z$

$$V_W(z,r,W,V_s,\beta) = C \cdot \sqrt{V_{rel}^2 + 2g(r-z)}$$

else

$$V_W(z,r,W,V_s,\beta) = 0$$

where

C	Inflow coefficient, taken as 1.0 in the presented results, (-)
V_{rel}	Relative velocity between water particles and ship, (m/s) $V_{rel} = V_s - V_{we} \cdot \cos(\beta)$
V_{we}	Horizontal velocity of the water particles, (m/s) (in the presented simulations, V_{we} is taken as a constant, 1.6 m/s representing an approximate average horizontal velocity).
g	acceleration of gravity, 9.8 m/s^2

The inflow coefficient C is difficult to estimate. In general it should be less then 1.0, but the open ramp may also have the effect of increasing the inflow rate. However, the presented results can be linearly scaled to any other estimated coefficient

Finally the frequency distribution of relative vertical motion is given by the Gauss- or Normal-distribution, here expressed as function of the significant relative motion rs equal to 2.0 times the standard deviation of the relative motion.

$$f_r(r,rs) = \frac{1}{(\frac{rs}{2})\cdot\sqrt{2\pi}} e^{-2\frac{r^2}{rs^2}}$$

The significant relative motion, rs, is a function of the ships speed, heading and amount of water, as well as of the mean wave period and the significant wave height

Since only the ramp opening was modelled, the water inflow simulation was stopped at the level when water started entering the C-deck. The final sequence of water ingress is deemed to be impossible to simulate with any accuracy.

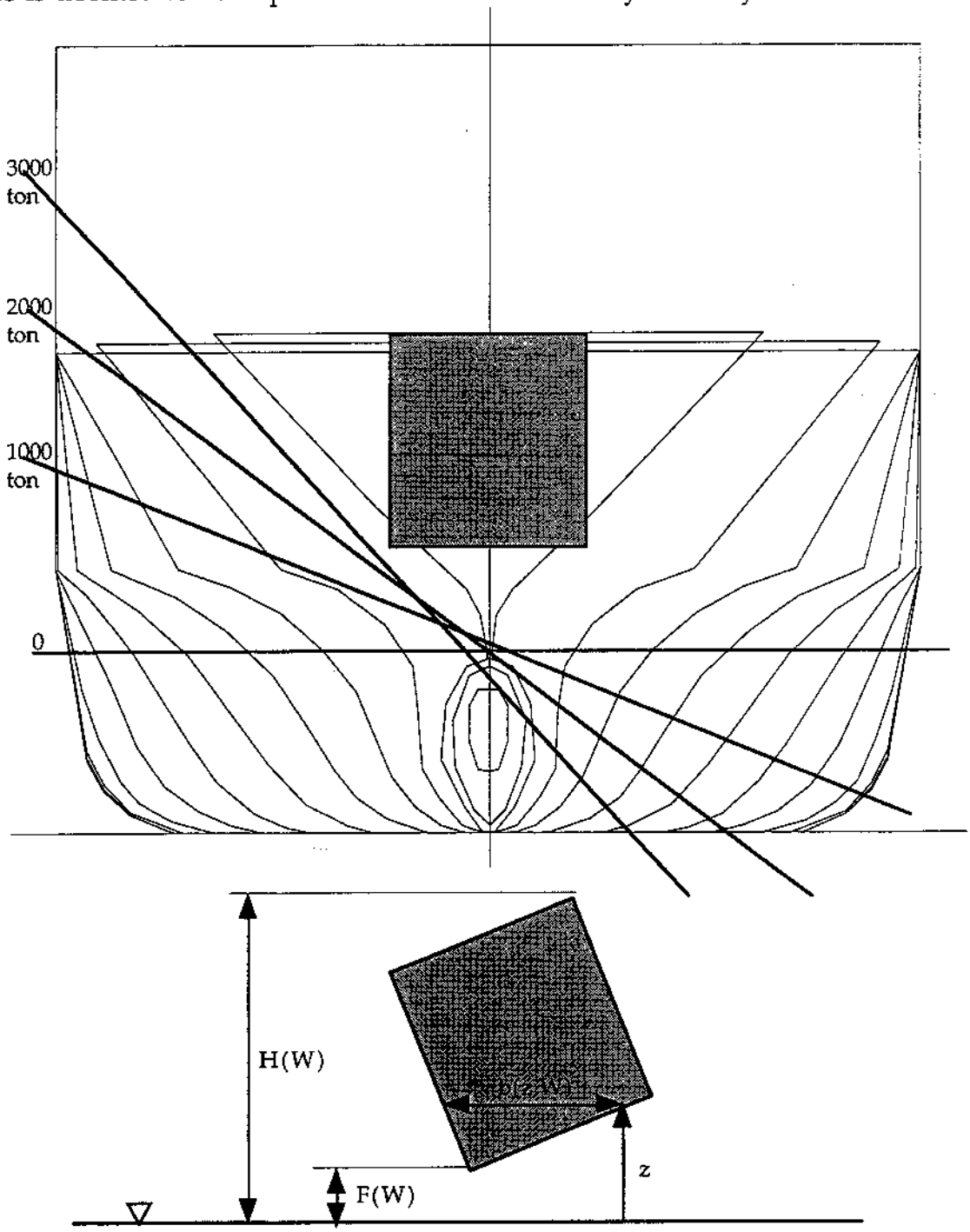

Figure 4.1 Examples of equilibrium water level for different amount of water on A-deck.Below is shown definition of geometry variables used in the general equation for calculation of water inflow.

4.2 Mean water inflow, example results

Calculated mean water inflow is given in Figures 4.2 - 4.8 as function of heading, speed and water on deck A. The three most important factors for the inflow is in decreasing order: the 'freeboard' distance F(W) from water level up to the opening, the significant relative vertical motion between ship and waves, rs, and the speed of the ship, V_S. They are however difficult to separate since the relative motion varies with the ship speed, and also the distance F(W) is affected by speed through the bow wave generated by the ship. The presented results include a bow wave correction on the mean water level estimated from the SHIPFLOW-calculations of the ESTONIA as given in Fig.3.7 of ref.[3]. Similar to the assumptions made in [4] this correction is taken as 1.0 m at 15 knots, 0.4 m at 10 knots and 0.2 m at 5 knots

In order to show more clearly and explicit the influence of different conditional parameters, Table 4.1 below has been prepared. However, it must be stressed that it is only a theoretical illustration. In the physical reality, all these parameters are coupled and will change in a much more complex way. For instance, at a constant displacement, an increased angle of heel will result in a decreased freeboard to the ramp opening. In the heel angle variation below, the F(W) has been kept constant and the inflow variation is only an effect of the rectangular geometry of the ramp opening.

Variation in speed (excl effect on bow wave and rs)

Vs (knots)	0	5	10	15	20
Qw (ton/min)	72	105	148	194	242

Variation in heading (excl effect on rs)

β (°)	60	90	120	150	180
Qw (ton/min)	112	125	138	148	151

Variation in 'freeboard'

F(W) (m)	1.5	2.0	2.5	3.0	3.5
Qw (ton/min)	475	273	148	75	36

Variation in heel angle (excl effect on freeboard and rs)

α (°)	0	10	20	30	40
Qw (ton/min)	148	84	55	42	38

Variation in relative vertical motion

rs (m)	2.5	3.0	3.5	4.0	4.5
Qw (ton/min)	25	71	148	254	387

Variation in water on C-deck,
(freeboard and heel variation included, rs constant)

W (ton)	0	200	400	700	1000
Qw (ton/min)	148	155	201	256	324

Table 4.1 Separate effect of different parameters on the calculated water inflow
The basic condition is: V_S = 10 knots, β = 150°, F(W) = 2.5 m, heel = 0°, rs = 3.5 m, W = 0 ton

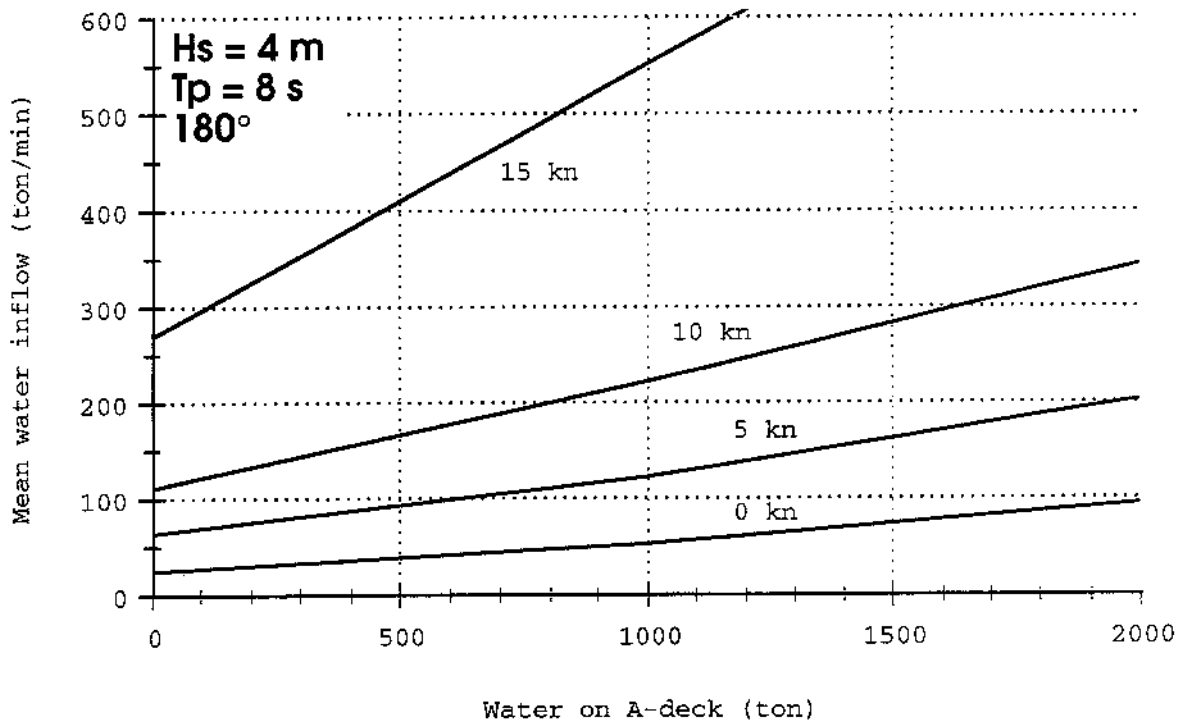

Figure 4.2 Mean water inflow as function of speed and amount of water on A-deck. Head sea 180°

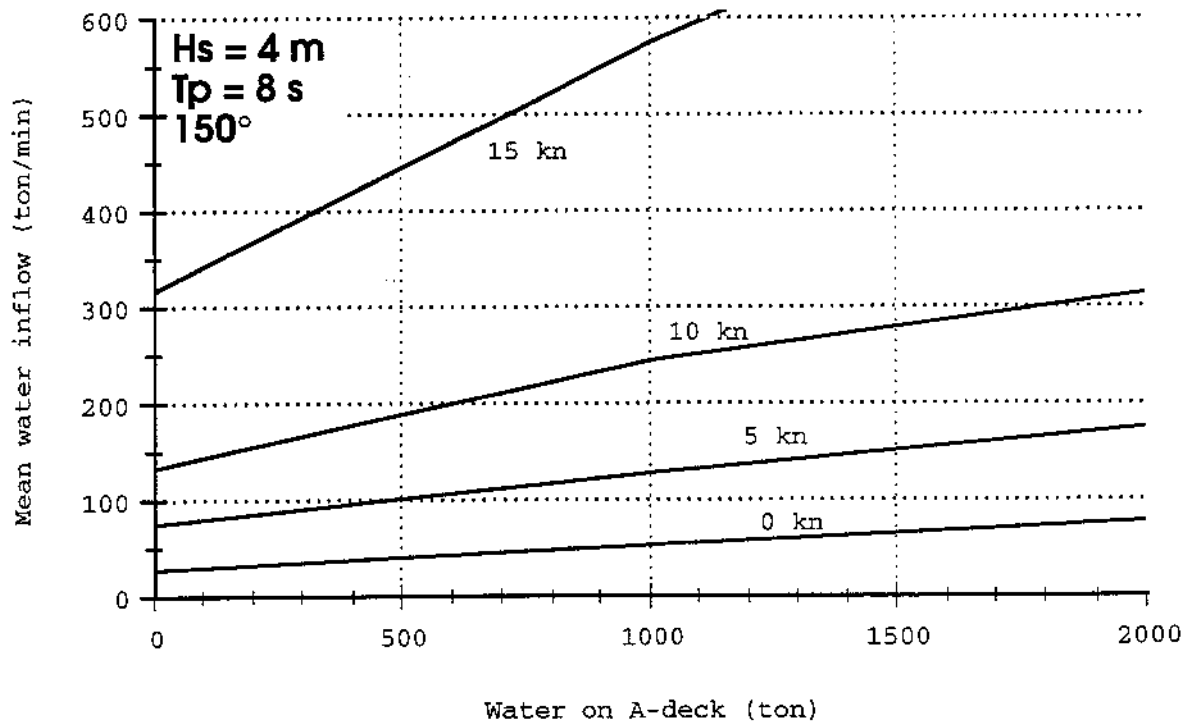

Figure 4.3 Mean water inflow as function of speed and amount of water on A-deck. Bow sea 150°

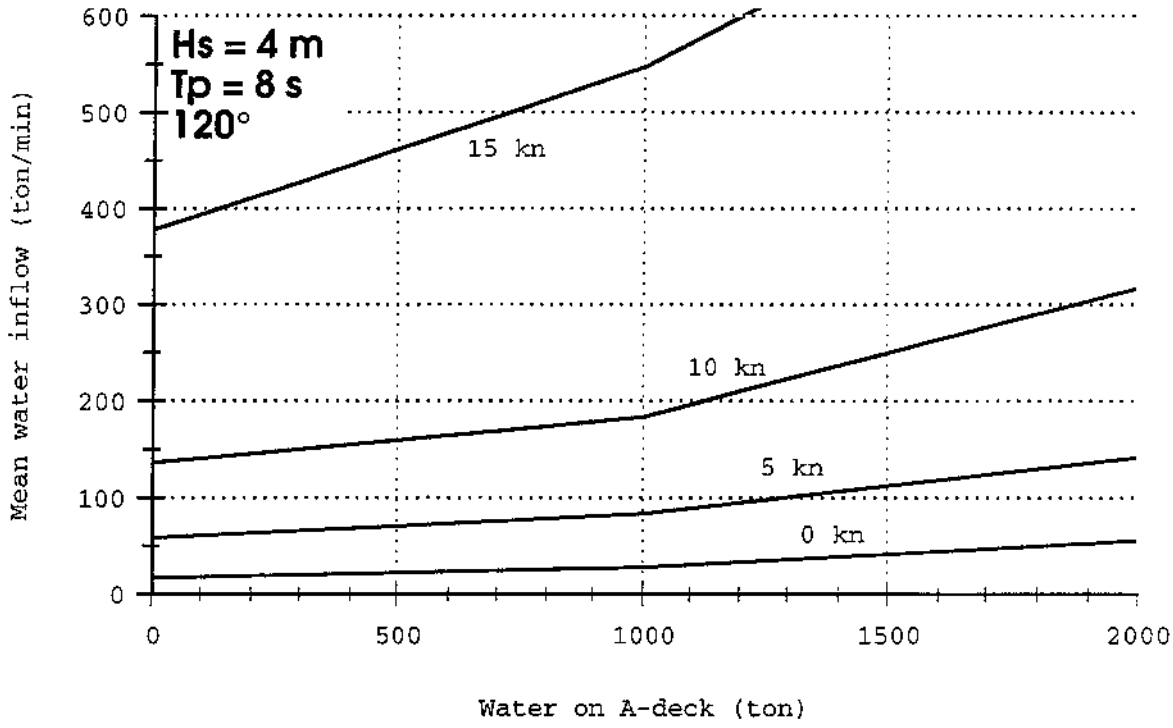

Figure 4.4 Mean water inflow as function of speed and amount of water on A-deck. Bow sea 120°

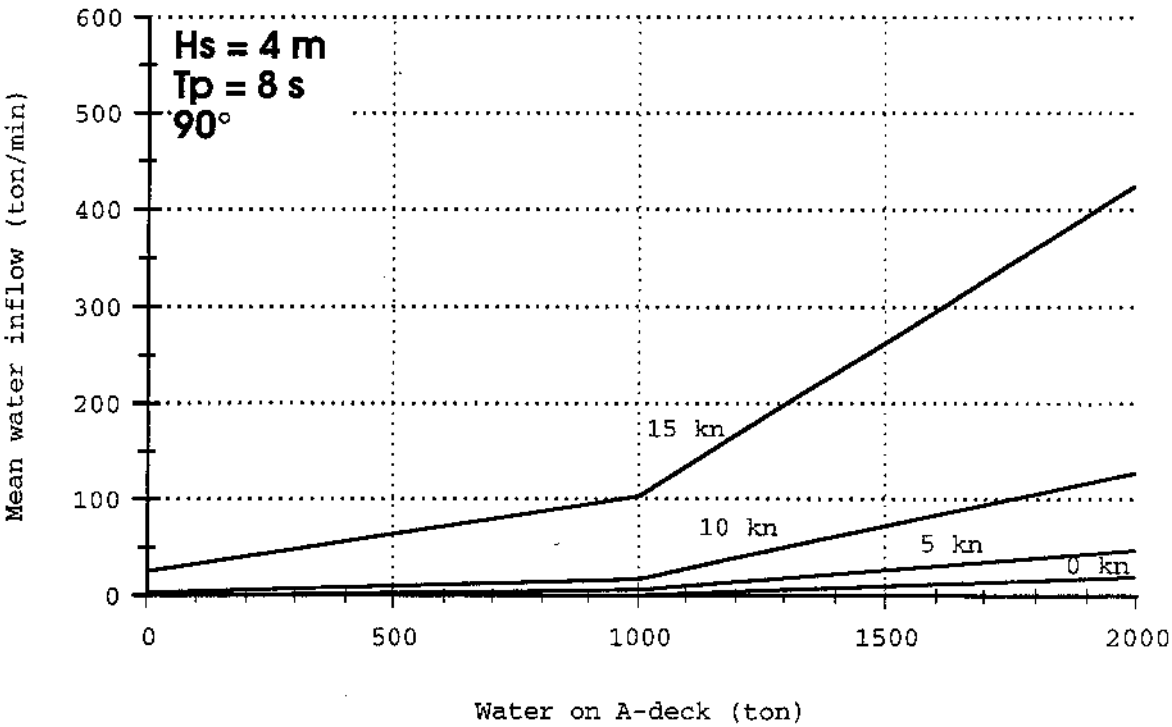

Figure 4.5 Mean water inflow as function of speed and amount of water on A-deck. Beam sea 90°

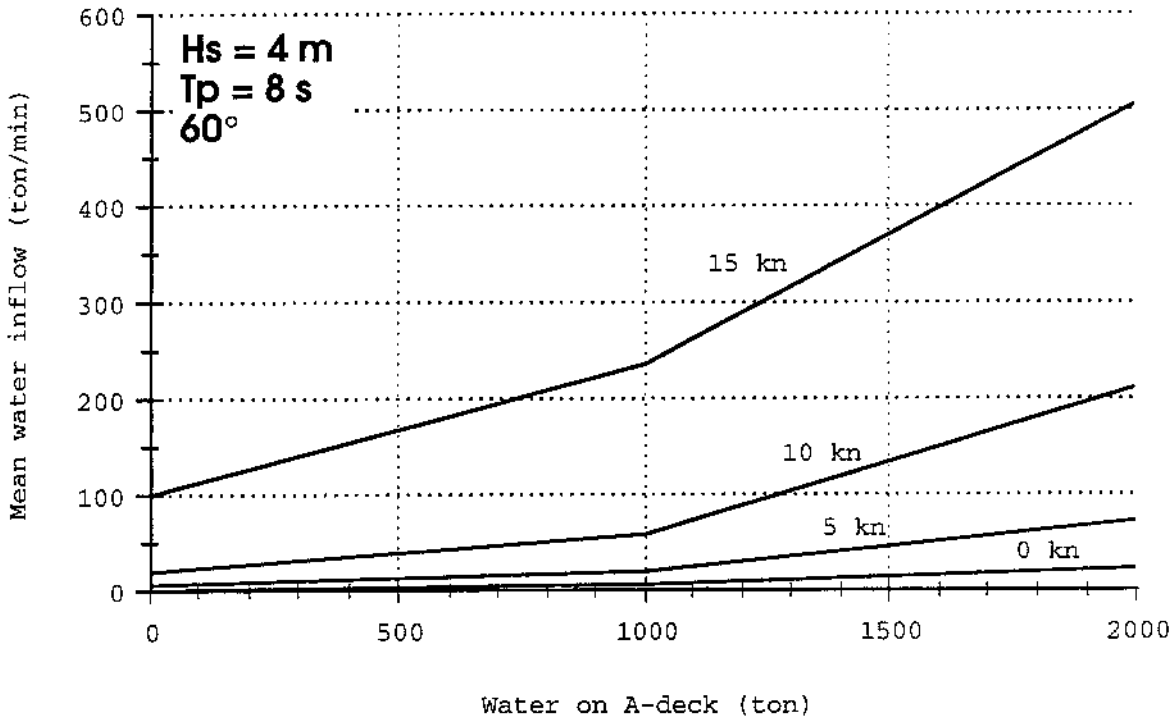

Figure 4.6 Mean water inflow as function of speed and amount of water on A-deck. Quarter sea 60°

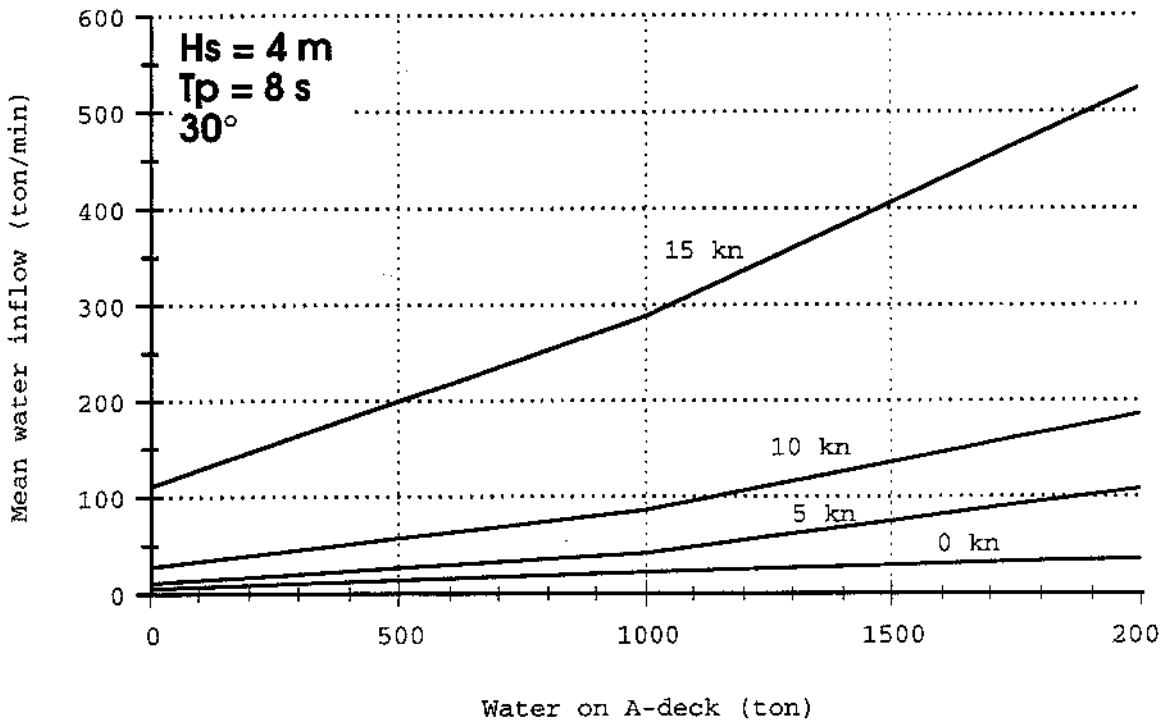

Figure 4.7 Mean water inflow as function of speed and amount of water on A-deck. Quarter sea 30°

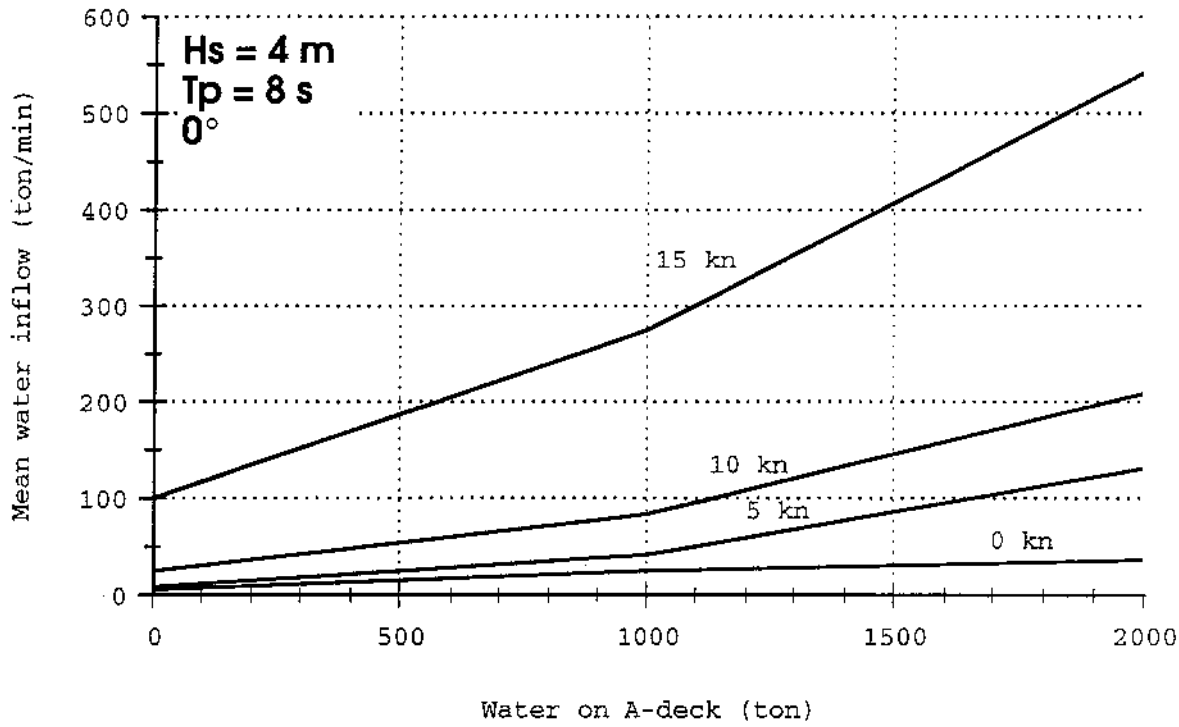

Figure 4.8 Mean water inflow as function of speed and amount of water on A-deck. Following sea 0°

4.3 Time sequence of water inflow

The amount of water on A-deck as function of time is obtained by integration.
In principle the governing equation can be expressed as:

$$W(t) = \int_0^t Q_W(W(t), V_s(t), \beta(t), rs(t))\, dt$$

Since W(t) is recursive in the expression, it has been solved with iterations in which the conditional parameters are adjusted to fit the time sequence results. The solution is therefore linked to an assumed general sequence of events with regard to the speed and heading of the ship. As a consequence there exist an infinite number of different possible solutions. In this report, only a few examples are given.

Example 1 A time sequence according to track simulations at Kalmar 1995

The first example is coupled to an early manoeuvring simulations of the ESTONIA during the last hour. This simulation was carried out at Kalmar Maritime Academy in order to find a possible track that could fit with the different positions of the bow visor and the wreck at the seabed. The simulation included the general manoeuvring characteristics of the ship and the effect of current and wind, but not directly the effect of heeling and wave motions. However, in an attempt to get as realistic conditions as possible, the projected area of the superstructure was continuously adjusted to account for the effect of heel on the wind drifting force.

The ship heading before the visor was lost was assumed to be 290° and the wave direction was assumed to be 245° which equals an initial relative heading to the waves of 135°.

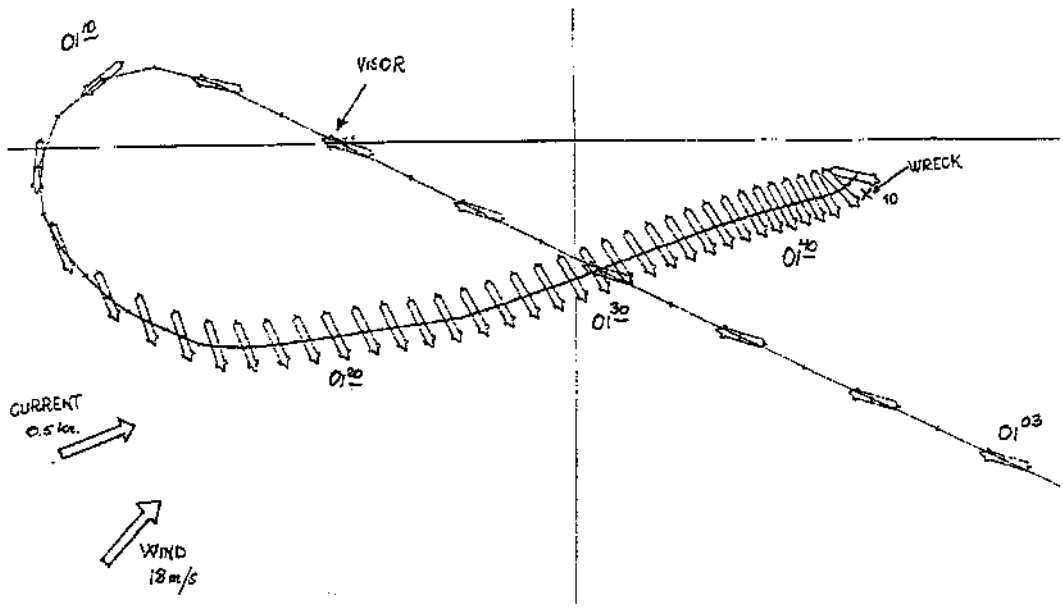

Figure 4.9 Plot of simulated track of the ESTONIA, Example 1.

Table 4.2 shows the different conditions used as base for the inflow simulation. The time, speed and heading fits approximately the sequence shown in Figure 4.9.

The result in terms of mean water inflow rate, accumulated water on A-deck and time is shown in Figures 4.10-4.11. According to this simulation it would have taken about a quarter of an hour from the first water ingress until larger amount of water started to enter the decks above car deck.

Time t (min)	Water W (ton)	Heel α (°)	Ship speed Vs (knots)	Rel Heading β (°)	Rel motion rs (m)	Sign Wave H Hs (m)	Wave period Tp (s)
0.0	0	0	14.5	135	3.5	4.1	8.0
0.6	200	6	14.5	135	3.5	4.1	8.0
1.4	400	11	11.5	150	3.5	4.1	8.0
2.7	700	17	9.0	-150	3.4	4.1	8.0
5.6	1000	22	3.0	-115	3.0	4.1	8.0
16.0	1500	29	0.0	-115	2.7	4.2	8.0
26.0	2000	37	0.0	-115	2.6	4.2	8.0

Table 4.2 Sequence of conditions in simulation example 1

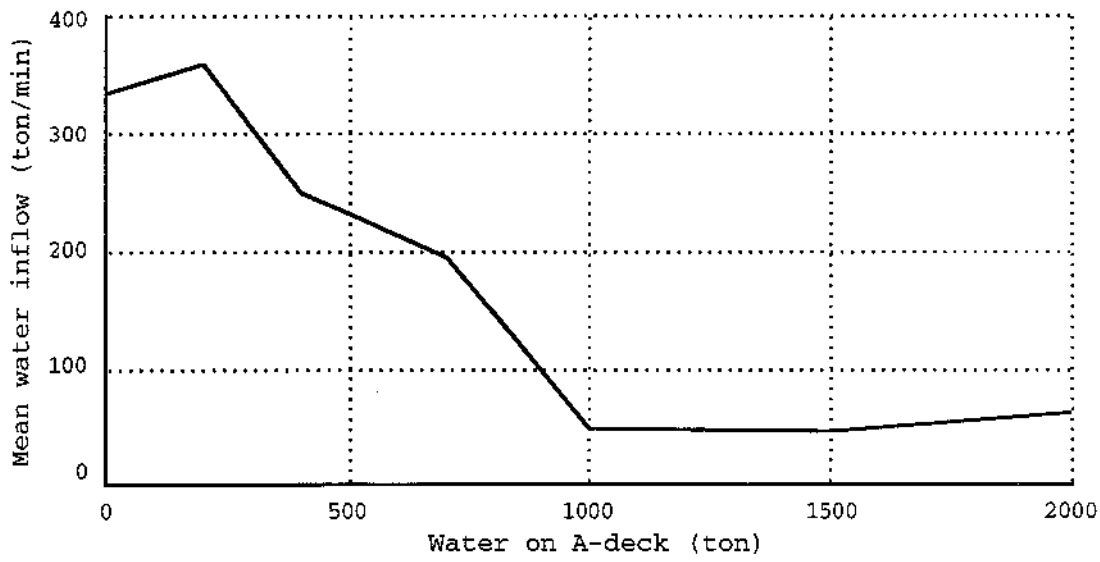

Figure 4.10 Mean water inflow per minute in simulation example 1.

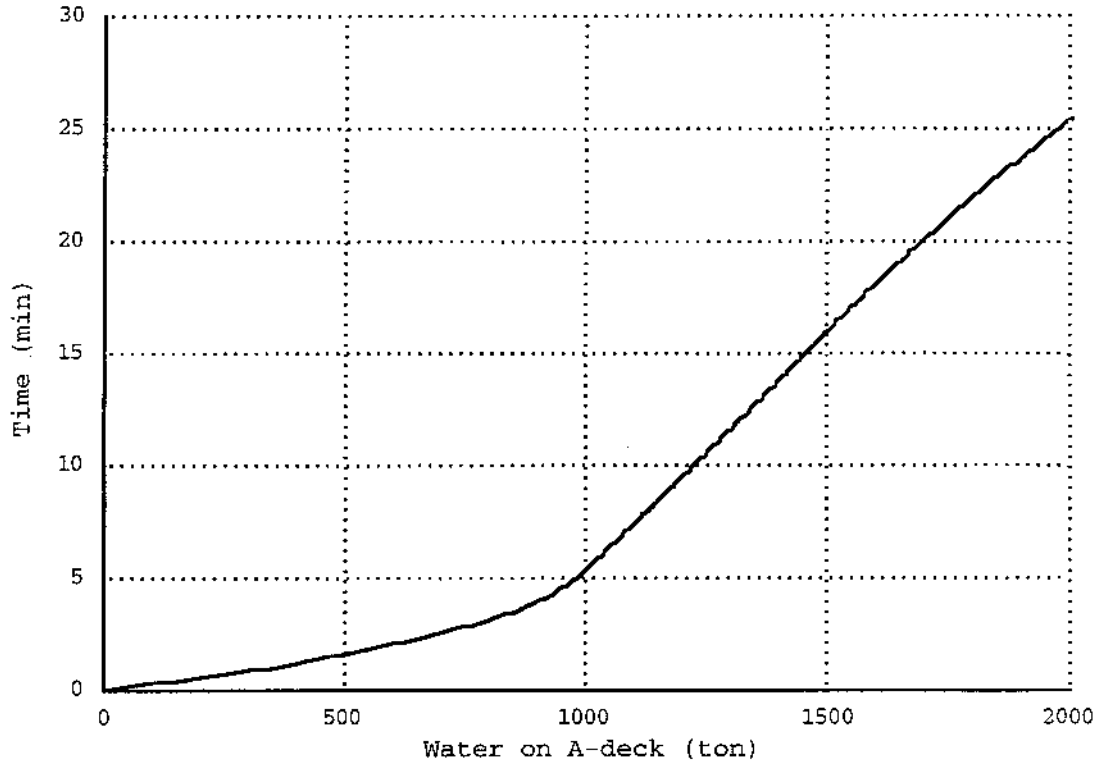

Figure 4.11 Time sequence of water inflow in simulation example 1.

Example 2 A time sequence according to track simulations at Kalmar 1996

This example is related to a later manoeuvring simulations of the track of ESTONIA. In this simulation the ship is assumed to have continued its course for about a minute after the ramp was opened. The speed was then reduced and a hard port turn was initiated. To fit the positions of the wreck and the visor on the seabed, the ship must have been running at low speed a few minutes on contra-course before the engines tripped and the ship started to drift with the sea on starboard beam. The simulated track is shown in Figure 4.12 and the assumed conditions in Table 4.3. The rate of inflow, and the accumulated water on deck is shown in Figures 4.13-4.14.

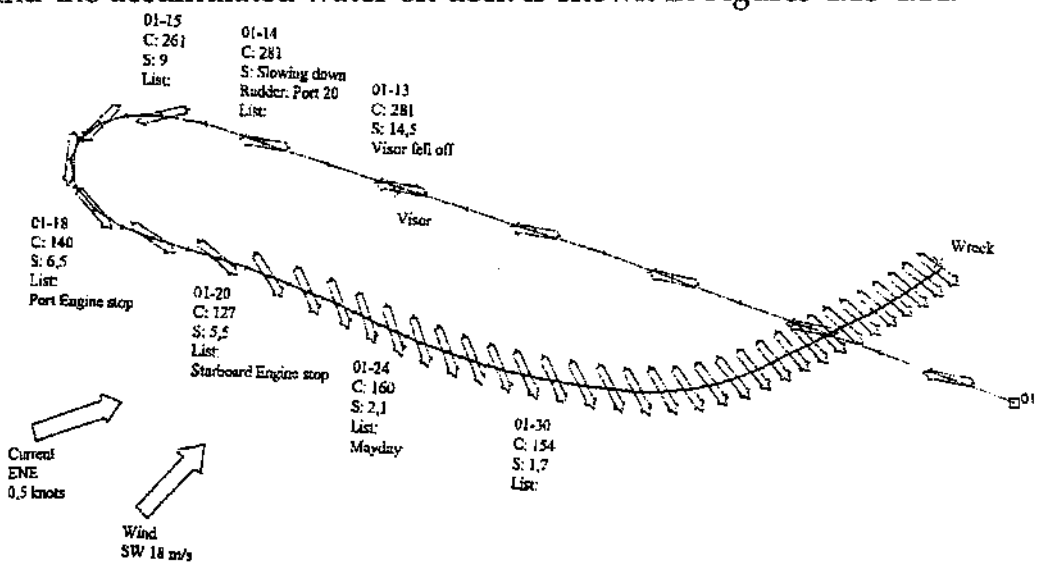

Figure 4.12 Plot of simulated track of the ESTONIA, Example 2.

Time t (min)	Water W (ton)	Heel α (°)	Ship speed Vs (knots)	Rel Heading β (°)	Rel motion rs (m)	Sign Wave H Hs (m)	Wave period Tp (s)
0.0	0	0	14.5	135	3.5	4.1	8.0
0.5	200	6	14.5	135	3.5	4.1	8.0
1.2	400	11	13.0	150	3.4	4.1	8.0
2.4	700	17	8.5	180	3.4	4.1	8.0
6.0	1000	22	5.5	-75	2.3	4.1	8.0
19.0	1500	29	0.0	-115	2.8	4.2	8.0
28.0	2000	37	0.0	-115	2.6	4.2	8.0

Table 4.3 Sequence of conditions in simulation example 2

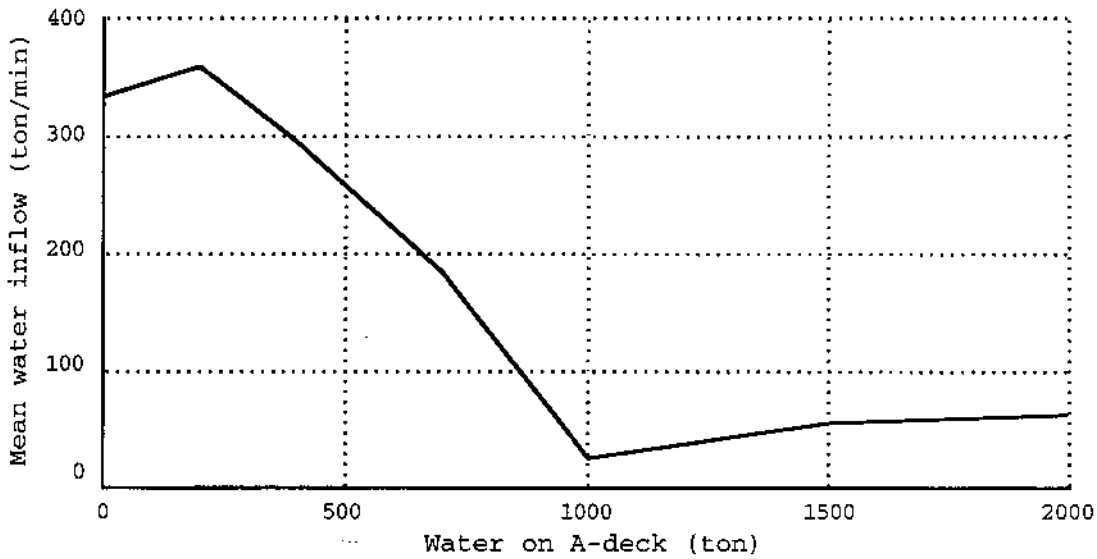

Figure 4.13 Mean water inflow per minute in simulation example 2.

Figure 4.14 shows that in this simulation the water inflow is slightly larger in the beginning of the sequence but significantly less 6-9 min after the ramp is opened. During this period the ship has completed the port turn and is running at 6 knots with close to beam seas. Such a plateau in the development of the list is also reported by witnesses but is stated to have occurred at a list of about 30°. If the ship in this simulation example had continued for about one more minute in bow or head sea, then the results would have fit these statements quite well, both with regard to the timing and to the development of the list.

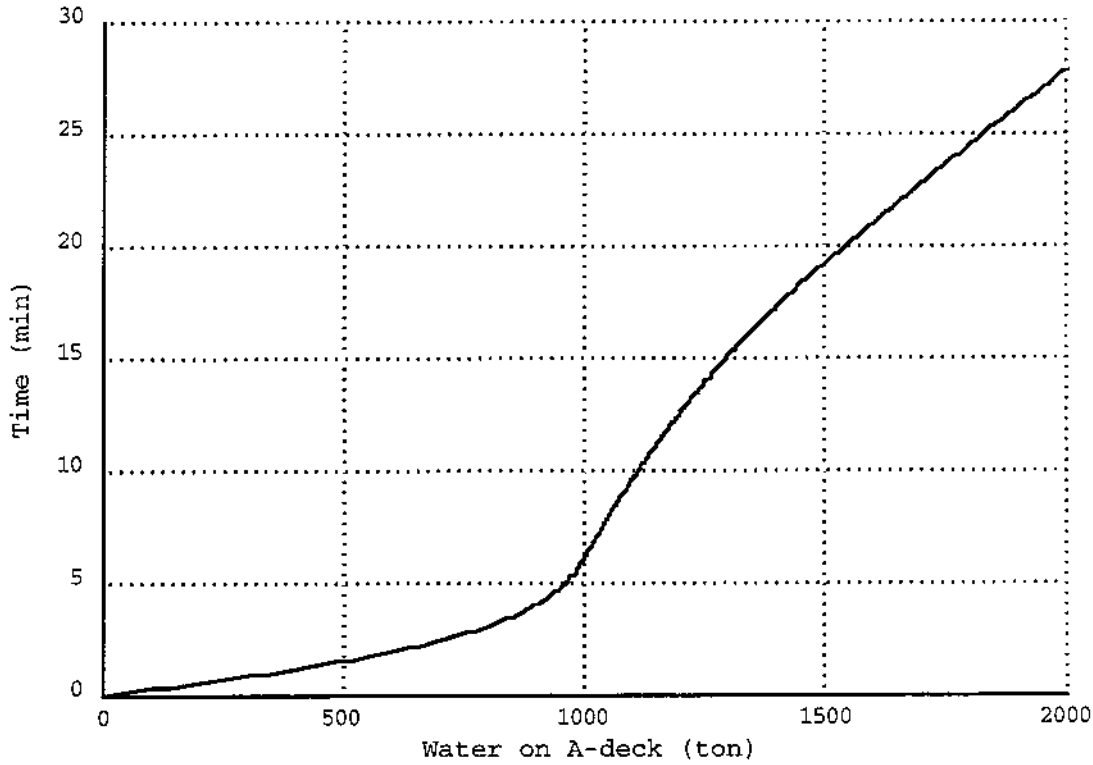

Figure 4.14 Time sequence of water inflow in simulation example 2.

Example 3 A hypothetic time sequence

Finally a hypothetical case has been simulated in order to illustrate what could have been the effect if the officers on bridge had been aware of the situation and had taken immediate actions in order to decrease the water inflow by decreasing speed and steering the ship to beam sea. The results indicate that there might have been a fair chance to save the ship if the heading was changed off the waves during the first critical minute. The simulation is however not very reliable since the random nature of seas and ship motions makes mean value estimates over just a few minutes very uncertain.

Time t (min)	Water W (ton)	Heel α (°)	Ship speed Vs (knots).	Rel Heading β (°)	Rel motion rs (m)	Sign Wave H Hs (m)	Wave period Tp (s)
0.0	0	0	14.5	135	3.5	4.1	8.0
0.7	200	6	13.0	120	3.5	4.1	8.0
2.0	400	11	5.0	90	2.2	4.1	8.0
70.0	700	17	0.0	90	2.2	4.4	8.0

Table 4.4 Sequence of conditions in hypothetic simulation example 3

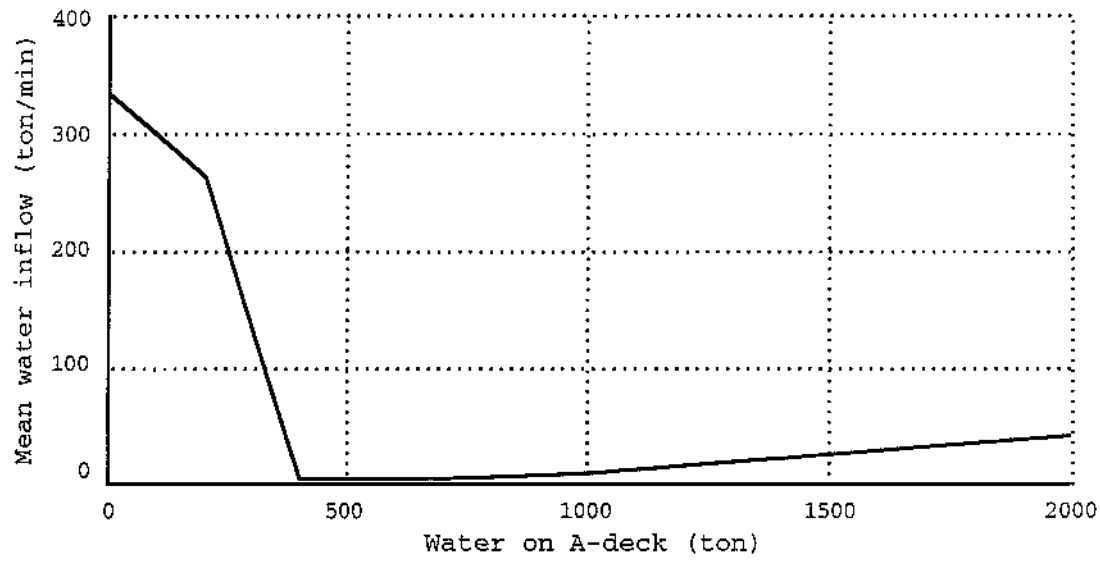

Figure 4.15 Mean water inflow per minute in hypothetic simulation example 3.

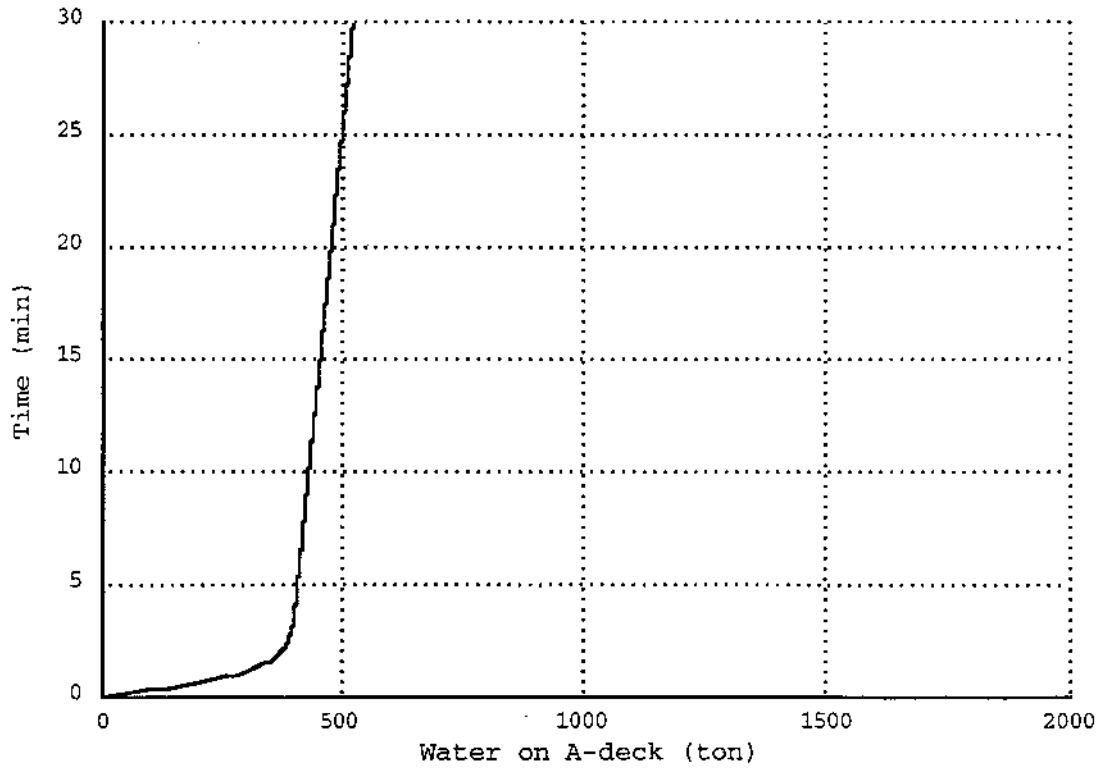

Figure 4.16 Time sequence of water inflow in hypothetic simulation example 3.

4.4 Comparison with time domain simulations at VTT, (4)

In ref [4] the water inflow has been predicted by using time series simulation instead of using the frequency distribution of relative motions as presented in this report. The principal differences between the two approaches are:

- The simulation in the time domain can take into account the actual velocity of water particles in each time step, while an average water velocity must be used in the frequency distribution approach presented in this report.

- The direct simulation makes it possible to predict the probability of exceedance of water inflow while the present simulation only can predict mean values of inflow.

Besides these principal differences there are also a number of other modelling differences between the two simulations.

- The relative motions in heeled condition has in [4] been calculated using the MOT35-program which is able to handle asymmetric hull shapes. In the present study, an ordinary strip-theory has been used with the submerged hull in heeled condition approximated as symmetrical, (Figures 3.2-3.3).

- In the time domain simulation, the irregular waves were assumed to be long-crested while the present study use relative motions calculated for a short-crested wave representation.

- The relative horizontal velocity and the inflow velocity due to hydrostatic pressure are treated separately and additive in [4], while in this study the two velocities are treated together according to the classical Bernoulli's equation (see e.g. Massey, Mechanics of Fluids, 3rd ed. eq (3.25)). In both simulations an inflow coefficient equal to unity has been used.

- Finally, the most important difference is that the still water freeboard at ramp opening in the VTT simulations were assumed to be 2.4 m while in this study it was calculated to be 2.97 m. This difference makes in general the calculated mean inflow in this report only half of what have been presented in [4] !

A comparison of results between the two approaches for mean values of water inflow is shown in the following Table 4.5. The table also includes results from the present approach but with separated horizontal velocities according to the VTT simulations. The same bow wave corrections on the freeboard, 1.0 m at 15 kn, 0.4 m at 10 kn, 0.2 m at 5 kn, 0.0 m at 0 kn, have been used in the comparison. The large difference is almost entirely caused by different assumptions of freeboard. The only exception to this are the values for 22° heel for which the MOT35 program gives much lower relative motions than for 0° or 35° heel and also much lower than those calculated approximately for 22° heel in this report.

If exactly the same condition is used, both approaches give also the same result of mean inflow, with differences of only a few percent, but it must once again be stressed that the simulations include many simplifications and uncertainties and the quantitative results should not be used uncritically.

If the higher inflow rates as given by the results from VTT would be used in simulation example 1 or 2, more than 1500 ton of water would enter the ship in two minutes. Such a rapid development of the list is not in accordance with witnesses statements.

				Mean water inflow [ton/min]		
Hs [m]	Vs knots	Heading [°]	Heel [°]	VTT approach ref [4]	Present appr.	Pres. appr. but sep. hor. veloc.
4	15	180	0	666	270	338
4	15	180	22	775	552	703
4	15	180	35/37	2078	829	1063
4	10	180	0	285	111	144
4	10	180	22	324	222	293
4	10	180	35/37	805	346	459
4	5	180	0	157	66	89
4	5	180	22	171	123	168
4	5	180	35/37	437	203	279
4	15	150	0	954	316	398
4	10	110/120	0	219	138	183
4	10	110/120	22	125	185	248
4	10	110/120	35/37	553	316	424
4	5	110/120	0	86	59	80
4	5	110/120	22	39	85	116
4	5	110/120	35/37	228	142	196
4	0	110/120	0	19	19	23
4	0	110/120	22	6	29	35
4	0	110/120	35/37	56	58	69
4	5	0	0	53	11	13
4	0	0	0	12	6	2

Table 4.5 Comparison of calculated mean water inflow by different methods and assumptions

5 References

[1] Karppinen T., Rantanen A., MV ESTONIA, Stability calculations, Technical Report VALC110, VTT, 1995

[2] Karppinen T., Rantanen A., MV ESTONIA, Numerical predictions of wave-induced motions, Technical Report VALC53, VTT, 1995

[3] Karppinen T., Rintala S., Rantanen A., MV ESTONIA, Numerical predictions of wave loads on the bow visor, Technical Report VALC106, VTT, 1995

[4] Rintala S., Karppinen T., MV ESTONIA, Numerical prediction of the water inflow to the car deck, Technical Report VALC174, VTT, 1996